HYBRID ANALYTICAL APPROACH COMBINING MORRICE AND LITTLE (DESIGN CURVE) WITH FINITE ELEMENT METHODS FOR ORTHOTROPIC BRIDGE DECKS

BY

JOSHUA, Oluwatoyin Raphael

ENG2006232

A PROJECT SUBMITTED IN

PARTIAL FULFILMENT OF THE REQUIREMENT FOR THE AWARD OF BACHELOR OF ENGINEERING (B.ENG).

IN

THE DEPARTMENT OF CIVIL ENGINEERING,

FACULTY OF ENGINEERING,

UNIVERSITY OF BENIN,

BENIN CITY, NIGERIA

NOVEMBER, 2025.

PLAGIARISM

This work **HYBRID ANALYTICAL APPROACH COMBINING MORRICE AND LITTLE (DESIGN CURVE) WITH FINITE ELEMENT METHODS FOR ORTHOTROPIC BRIDGE DECKS** by **JOSHUA, Oluwatoyin Raphael** with Mat Number **ENG2006232** of the Department of Civil Engineering, Faculty of Engineering, University of Benin, Benin City, Edo State, Nigeria, has PASSED the PLAGIARISM TEST.

PROJECT COORDINATOR

Name: Engr. E. ORIA-USIFO

Signature and Date: .....

CERTIFICATION

This work was carried out by Joshua Oluwatoyin Raphael, Mat No. ENG2006232, of the Department of Structural Engineering, University of Benin, Benin City, Edo State, Nigeria and is hereby certified.

PROJECT SUPERVISOR

Name: ENGR. (DR.) MUSA AARON

Signature: …… Date: ……..

HEAD OF DEPARTMENT

Name: ENGR. PROF. (Mrs.) N. I. IHIMEKPEN

Signature: …… Date: ……..

DEDICATION

This project is dedicated to GOD Almighty, to my Father and Mother, MR and MRS JOSHUA and to my entire family members for their love, contributions and sacrifices to my education.

ACKNOWLEDGEMENT

This project has been made possible by the blessings of Almighty God for His strength, wisdom, and guidance.

The work would not have been accomplished without the supervision from ENGINEER MUSA AARON for his valuable support, and constructive criticism which shaped the quality of this work alongside his guidance and research encouragement.

Also, A special thanks to the Head of Department, Prof. Ngozi Ihimekpen for her leadership role, also my course adviser Engr. Nosa Kent and all the lecturers and staff in the department of Civil/Structural Engineering. Prof. O.U Orie, Prof .H.A.P Audu, Engr. Prof. R.O. Ogirigbo, Engr. Prof. J.O. Okovido, Engr. Dr. P.N. Ogbuefun, Engr Dr. A. Rawlings, Engr, Engr E. A. Agabi, Engr. E. Oria Usifo.

My major appreciation goes to my wonderful parents, Mr. and Mrs. Joshua, and my entire family members, who were always there for me.

Your encouragement and love, my dear friends, has made this journey a remarkable one and I appreciate the faith that you placed in me. I am truly blessed to be surrounded by family members whose unwavering support has served as my pillar.

My gratitude also extends to all my people and organisations who supported and motivated my work in one way or another. Your presence in my life has played a big part of my student's life journey.

ABSTRACT

This study aimed to develop and validate a hybrid analytical framework for the structural analysis of orthotropic steel bridge decks, particularly those with skewed or curved geometries. The primary goal was to improve the accuracy of load distribution and force prediction by integrating the classical Morrice and Little (M-L) design curve method with a finite-element orthotropic-plate model within a MATLAB environment. The study was motivated by the need to reduce the limitations of purely empirical approaches and the computational burden of full-scale 3D finite element (FE) analysis, offering an efficient yet accurate alternative for early and intermediate stages of bridge design.

The methodology involved extracting detailed geometric and material data from a 30 m long, simply supported orthotropic bridge deck modelled in STAADPro v8i, including 3 main girders (W900 × 300 mm), 12 mm thick longitudinal ribs spaced at 300 mm, and 2 m cross-girder spacing. Flexural rigidities (Dx, Dy), torsional constant ($\alpha = 0.45$), and skew factor ($\theta = 0.789$) were calculated and used in a finite-difference orthotropic plate model (1 m × 1 m mesh with simply supported boundaries). Load effects from a 300 kN HB axle (with a 1.25 impact factor) were applied at mid-span. MATLAB was used to interpolate M-L distribution coefficients, integrate them with global stiffness matrices, and perform moment and deflection analysis. Comparative validation was performed against detailed shell-element results from STAADPro.

Numerical results showed that the hybrid model predicted peak girder bending moments of 5951KNm, closely matching the STAADPro value of 5850KNm, with an error margin of just 1.7%. The mid-span deflection was 19.4 mm, only 2.6% higher than the STAAD result (18.9 mm), and well within the L/500 deflection limit of 60 mm. In contrast, the classical M-L method predicted a more conservative moment of 5380KNm, 8% lower than STAAD. Computational efficiency was significantly improved: MATLAB solved each case in under 0.8 seconds, compared to 45 seconds per case in STAADPro, demonstrating a 50× speed-up. These findings confirmed that the hybrid approach offers a code-compliant, accurate, and computationally efficient solution for the analysis of orthotropic bridge decks, reducing over-design and enabling faster design cycles.

SUMMARY OF WORK

This work presents a hybrid analytical methodology that integrates the Morrice & Little design curve approach with Finite Element (FE) analysis to improve the structural assessment of orthotropic bridge decks, particularly those with skewed or curved geometries. The Morrice & Little method, a simplified and efficient design curve technique, provides rapid estimations of the deck's structural response based on empirically derived relationships. However, its accuracy diminishes for complex geometries such as skewed or curved decks where three-dimensional effects and anisotropic behaviors play a significant role.

To address these limitations, the proposed approach couples this simplified method with detailed finite element modeling, leveraging MATLAB's computational capabilities. The FE analysis accounts for the orthotropic material properties, geometric irregularities, and boundary conditions, enabling precise simulation of stress distribution and deformation patterns in complex deck configurations. MATLAB's matrix computation techniques facilitate efficient data handling, model setup, and result post-processing.

The hybrid methodology starts with the Morrice & Little design curve to obtain initial estimates of the deck's structural performance, which are then refined through FE analysis. This combination ensures a balance between computational efficiency and accuracy, especially for skewed and curved decks that challenge conventional simplified models. Ultimately, this integrated approach aims to provide engineers with a practical and reliable tool for the structural evaluation, optimization, and safety assessment of orthotropic bridge decks with complex geometries, enhancing both design precision and computational efficiency.

TABLE OF CONTENT

Title Page	i
Plagiarism	i
Certification	ii
Dedication	iii
Acknowledgement	iv
Abstract	v
Table Of Content	vi
List Of Tables	x
List Of Figures	xii
CHAPTER ONE: INTRODUCTION	**1**
1.1 Background of Study	1
1.2 Statement of The Problem	4
1.3 Aim and Objective of The Study	5
1.4 Scope of Study	6
1.5 Justification of Study	7
CHAPTER TWO: LITERATURE REVIEW	**9**
2.0.1 Element types	9
2.0.2 Mesh sizing	11
2.1 Orthotropic plate	11
2.2 Structural components of Orthotropic Bridge Deck	12

2.2.1 Wearing surface 12

2.2.2 Deck plate 13

2.2.3 Longitudinal stiffeners 13

2.2.4 Transversal stiffeners 17

2.3 Orthotropic Plate Theory 17

2.3.1 The theory of Guyon and Massonnet 20

2.4 Morrice and Little Design Curve Method in Bridge Deck Analysis 20

2.5 Finite element method for Orthotropic Bridge Decks 21

2.6 Finite element modelling 22

2.7 Finite Element Modelling Techniques 23

2.8 Integration of Morrice and Little with Finite Element Analysis 24

2.9 Role of MATLAB and Matrix Computation Techniques 25

2.10 Accuracy and Practical Benefits 25

2.11 Conclusion of Literature Review 25

CHAPTER THREE: METHODOLOGY **26**

3.1 Study Area 26

3.2 Procedures and Methods of Analysis 27

3.2.1 The Morrice and Little Design Curve Method 27

3.2.2 Finite Element Modeling in MATLAB 28

3.2.2.1 Model Development 28

3.2.2.2 Incorporation of Material Anisotropy 28

3.2.2.3 Loading and Boundary Conditions 29

3.2.2.4 Analysis and Solution 29

3.2.2.5 Validation and Comparison 29

3.3 Integration of Methods 29

3.4 Implementation in MATLAB 30

3.4.1 Mesh Generation 30

3.4.2 Material Property Definition 30

3.4.3 Stiffness Matrix Assembly 30

3.4.4 Applying Loads and Boundary Conditions 30

3.4.5 Solution 30

3.4.6 post-processing 30

CHAPTER FOUR: RESULTS AND DISCUSSION 36

4.1 Introduction 36

4.2 Results from Finite Element Analysis (STAAD pro Design) 36

4.3 Results from Morrice and Little Design Curve Approach 58

4.3.1 Analysis and Design of Deck Slab 58

4.3.2 Load Calculation 60

4.3.3 Analysis of Slab 65

4.3.3.1 Check for Ultimate Limit State 66

4.4 MATLAB Code Project File 69

4.4.1 MATLAB Input Parameters and Geometry 69

4.4.2 Section Property Calculations 69

4.4.3 Morrice and Little Load Distribution 70

4.4.4 Finite Element Modelling 70

4.4.4.1 Mesh Generation and Plate Stiffness Assembly 70

4.4.4.2 Load Application and Boundary Conditions 70

4.4.5 Bending Moment Comparison 71

4.4.6 Plots and Diagrams 71

4.4.7 Custom Functions 72

CHAPTER FIVE: CONCLUSION AND RECOMMENDATION 73

5.0 Conclusion 73

5.1 Recommendations 74

REFERENCES 75

LIST OF TABLES

Table 3.1: Notional Lanes for design purposes according to the carriageway width 31

Table 3.2: HA Loading 31

Table 3.3: HA lane factors 32

Table 4.1: Section Properties 37

Table 4.2: Plate Thickness 37

Table 4.3: Material Properties 37

Table 4.4: Primary Load Cases 38

Table 4.5: BS5400: SLS BS5400_Gen_Load N39: Disp Y -ve: Plate Loads 39

Table 4.6: BS5400: SLS BS5400_Gen_Load N39: Disp Y -ve: Plate Loads 40

Table 4.7: BS5400: SLS BS5400_Gen_Load N41: Disp Y -ve: Plate Loads 41

Table 4.8: BS5400: SLS BS5400_Gen_Load N42: Disp Y -ve: Plate Loads 42

Table 4.9: BS5950: Load Factor of Safety 43

Table 4.10: Node Displacements Summary 43

Table 4.11: Node Displacements Summary 44

Table 4.12: Node Displacements Summary 44

Table 4.13: Plate Centre Stress Summary 45

Table 4.14: Plate Center Principal Stress Summary 46

Table 4.15: Reaction Summary 47

Table 4.16: Beam End Displacement Summary 48

Table 4.17: Reaction Envelope 49

Table 4.18: Bridge Geometry and Material Properties 59

Table 4.19: Bridge Geometry and Material Data Input 63

Table 4.20: Slab Design Moment from Staad Analysis 63

Table 4.21: Reinforcement Schedule from Staad Analysis 65

Table 4.22: Moment of Resistance (MOR) Check from Staad Analysis 65

Table 4.23: SLS Rare Steel Stress Check from Staad Analysis 65

Table 4.24: SLS QP Steel Stress Check from Staad Analysis 66

Table 4.25: Crack Width Check from Staad Analysis 66

LIST OF FIGURES

Figure 1.1: Principal layout of an orthotropic bridge deck. 2

Figure 2.1: Structural elements 10

Figure 2.2: Difference btw linear and higher order elements for a 4-node element 10

Figure 2.3: Difference between full and reduced integration. 11

Figure 2.4: Closed and open Rid 14

Figure 2.5: Amount of welding required in open and closed ribs (Karlsson, 2015) 16

Figure 2.6: Bridge geometry in FE-model. 23

Figure 3.1: The cross-section of the composite bridge deck. 26

Figure 3.2: Loading curve HA UDL (Not to scale) 32

Figure 3.3: HB Vehicle 34

Figure 3.4: A combination of HA and HB loading: HB within one notional lane 34

Figure 3.5: A combination of HA and HB loading; HB for two notional lanes 35

Fig 4.1: Bending Moment transverse and longitudinal stress diagram 54

Fig 4.2: Bending Moment and Shear Force for transverse and longitudinal beam 54

Fig 4.3: Bridge Deck showing HA and HB loading range (MPa) 55

Fig 4.4: Bridge Deck showing HA and HB loading roadway 55

Fig 4.5: 2D View of Bridge Deck 56

Fig 4.6: 3D View of Bridge Deck 57

Fig 4.7: 3D View of Bridge Deck 58

Fig 4.8: 3D Modelled structure of Bridge Deck on Staad Pro 59

Fig 4.9: Transverse and Longitudinal stress on Bridge Due to Dead Load 60

Fig 4.10: Maximum Transverse and Longitudinal stress on Bridge 61

Fig 4.11: Comparison of BMD Using Morrice-Little and FEM Methods 71

CHAPTER ONE

INTRODUCTION

1.1 Background of Study

This research studies the development of a hybrid analytical framework that combines the Morrice and Little design curve method with finite element analysis, thereby improving the precision of assessments for Orthotropic Bridge Decks (OBD) with complex geometries.

Bridges are construction designed to carry road traffic and other moving loads over obstacles, enabling the passage of pedestrians, vehicles, trains, canals, pipelines and more. These obstacles can include natural features such as rivers, valleys, and sea channels or man-made structures like other bridges, buildings, railways and roads. Even though a typical standard bridge is less complex, (two supports holding up a beam) even in this simplified form, bridges experience its engineering challenges. The support must be sufficiently strong enough to support the structure and the span between must be durable enough to withstand the loads. (Kanwarjot 2023)

Among the various bridge types, orthotropic bridge decks have gained prominence due to their lightweight constructions, high strength-to-weight ratio, and adaptability to complex geometrics such as skewed or curved configurations. The vast majority of the world bridges with a record of long spans have utilized orthotropic bridge decks. The (OBD) decks, typically composed of steel plate stiffened with longitudinal ribs and transverse diaphragms, exhibits orthogonal-anisotropic behavior which is shortened “orthotropic” meaning their mechanical properties vary with direction. This orthotropic nature complicates their structural analysis, particularly under dynamic and live loads, necessitating advanced methodologies to ensure accurate design and performance evaluation (Hibbeler, 2016). Historically, bridge engineering has relied on empirical

techniques and simplified analytical model to guide design. The evolution of bridge deck analysis can be traced back to the early 20th century when engineers relied on simplified beams theory and empirical formulas to design structures. The introduction to orthotropic decks in the mid-20th century, notably with the pioneering work of Cornelius and Huber in the 1950s, marked a very significant advancement.

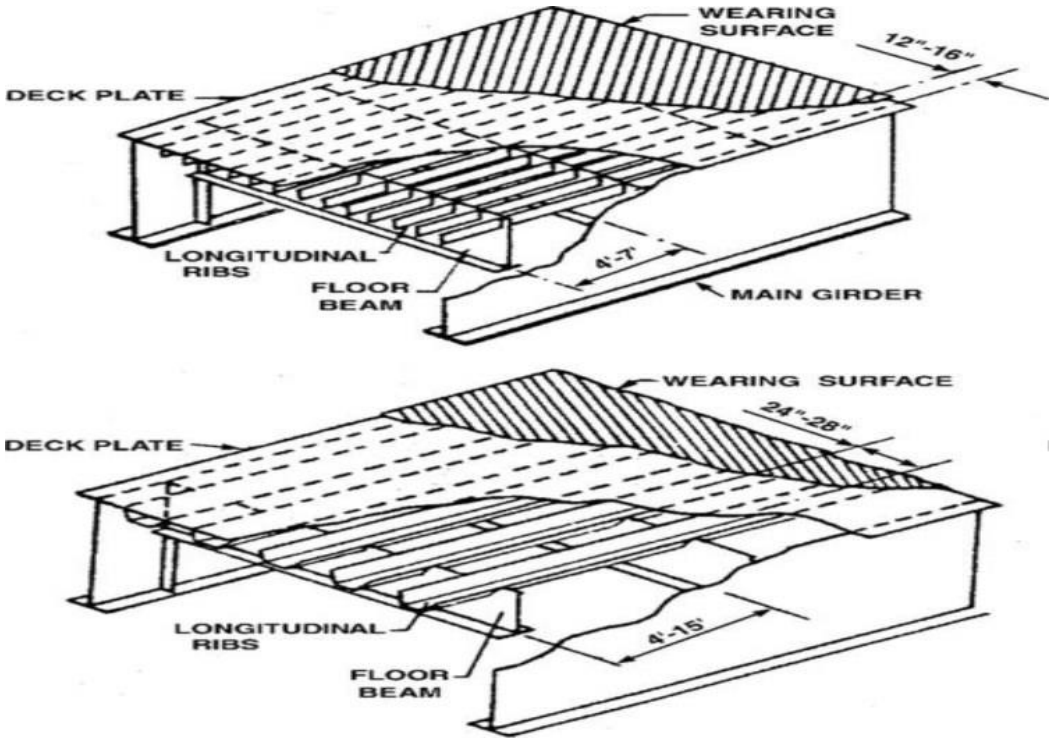

Figure 1.1: Principal layout of an orthotropic bridge deck.

The design and analysis of bridge decks are crucial components in structural engineering, ensuring safety, durability, and cost-effectiveness. Traditional analytical methods, such as the Morrice and Little (Design Curve) approach, provide simplified means for assessing the load-carrying capacity of orthotropic bridge decks (Morrice and Little, 1954). These methods are valued for their efficiency and ease of application but often lack the precision needed for complex geometries, such as skewed or curved decks, which are increasingly common in modern bridge construction due to aesthetic and structural considerations. Conventional methods may fall short in providing detailed stress and deformation estimates in such cases, leading to potential safety concerns or

over-conservatism, which increases costs.

Finite Element Methods (FEM) have revolutionized structural analysis by enabling detailed simulation of complex geometries and material behaviors (Zienkiewicz and Taylor, 2005). Finite Element Method (FEM) allows for the precise modeling of orthotropic decks, capturing nuanced stress distributions rather than relying on simplified assumptions. However, FEM can be computationally intensive and requires significant expertise, limiting its routine application in preliminary design stages. To bridge the gap between efficiency and accuracy, recent research has explored hybrid approaches that combine classical design methods with modern computational techniques. Integrating the Morrice and Little design curve with FEM offers a promising avenue to refine the analysis of skewed and curved bridge decks, leveraging the strengths of both methods. MATLAB, with its robust matrix computation capabilities, serves as an ideal platform for implementing such an integrated approach, facilitating efficient and accurate analysis (MathWorks, 2023).

This approach intends to optimize safety, accuracy, and computational efficiency, advancing current practices in bridge engineering.

1.2 Statement of The Problem

The structural analysis of orthotropic bridge decks, particularly those with skewed or curved geometries, presents significant challenges due to their complex material behavior and geometric configurations. Conventional analysis methods, such as the Morrice and Little design curve approach, offer simplified solutions that are efficient for routine assessments but often lack the accuracy needed for modern, intricate bridge designs (Morrice and Little, 1954). These methods assume idealized conditions that do not fully capture the stresses and deformation patterns in complex geometries, potentially leading to unsafe designs or over-conservative estimates, which result in unnecessary material usage and increased costs.

Finite element method (FEM), on the other hand, can provide detailed insights into the stress distribution and overall behavior of orthotropic decks with complex geometries (Hibbeler, 2016). However, FEM is computationally intensive and requires significant expertise, limiting its utility in preliminary design phases or routine assessments. This creates a gap in the existing methodologies: there is no integrated approach that combines the efficiency of classical methods with the accuracy of detailed numerical analysis to evaluate complex orthotropic decks effective.

The core question this research seeks to answer is: Can a hybrid analytical approach that combines the Morrice and Little design curve method with finite element analysis improve the accuracy and efficiency of orthotropic bridge deck assessment, especially for skewed or curved geometries? Addressing this question is vital for enhancing the safety, cost-effectiveness, and practicality of bridge design and evaluation.

1.3 Aim and Objective of The Study

The main aim of this project is to develop a Hybrid Analytical Approach of Combining Morrice and Little (Design Curve) as well as FEM for the improvement of load distribution and force prediction accuracy on skewed or curved orthotropic bridge decks, which will be achieved through the application of MATLAB.

The specific objectives are to:

1. To study and model the load distribution behaviour of orthotropic bridge decks using Morrice and Little design curve approach and Finite Element Method focusing on flexural their limitation in analyzing complex geometries.
2. Integrate the approaches algorithmically in MATLAB, with matrix computations marrying design curve coefficients with FEM stiffness and load matrices for global analysis.
3. Validating the hybrid model through comparison with benchmark bridge cases and other software result such as Staad Pro v8i.
4. To formulate and document the findings, including the development of guidelines for the design and analysis of orthotropic bridge decks using the hybrid approach

1.4 Scope of Study

The research integrates the Morrice and Little design curve approach with finite element analysis to develop, implement, and validate a hybrid analytical model for evaluating orthotropic bridge decks, particularly those with complex geometries like skewed or curved configurations. This comprehensive study includes a literature review of classical design methods and finite element modeling techniques for orthotropic bridge decks, specifically examining their strengths and weaknesses when applied to skewed and curved geometries. It will identify and define crucial parameters such as geometric configurations (e.g., skew angles and curvature), orthotropic material properties, loading conditions, and boundary constraints.

A computational model will be developed in MATLAB, combining the foundational Morrice and Little design principles with advanced finite element analysis techniques. This hybrid model will then be applied to analyze various bridge deck configurations, with a specific focus on skewed and curved geometries, for span lengths ranging from 10 to 30 meters under highway loads like HA and HB loading.

1.5 Justification of Study

This project presents the design and analysis of an Orthotropic Bridge Deck structure, combining both manual design techniques and software-based analysis. While extensive research has been conducted on bridge design and analysis, very few studies have specifically explored the integration of manual design methods with software-driven optimization, particularly for orthotropic bridge decks.

The primary aim of this research is to assess the reliability, efficiency, and performance of orthotropic bridge deck systems and to support their design through the development of a user-friendly based design tool that will enable engineers to: Automatically analyse the structural behaviour of orthotropic bridge decks, Optimize the deck configuration for improved structural performance and material efficiency. By combining manual design checks with advanced computational analysis, this project seeks to enhance both the accuracy and accessibility of orthotropic bridge deck design.

Orthotropic bridge decks have gained popularity in recent years due to their unique structural properties and advantages over traditional bridge deck designs. Here are some key factors contributing to their popularity: The OBD is an efficient and economic system because the deck acts as top flange for the longitudinal and the transversal stiffeners as well as for the main girders (US Department of Transportation, 2012). This means that material is saved and it also increases the rigidity of the deck. The leading benefit of the Orthotropic Bridge Decks system is the minimization of dead load in the design and the rapid construction that tends to lessen the impact on traffic. Modern practice, however, relies heavily on detailed finite element (FE) models. Indeed, “Most bridges today are designed using finite element method,” albeit with caution since orthotropic decks are so complex that engineers still use simplified models and hand calculations alongside them

The Morrice and Little method remains a respected traditional tool for analyzing orthotropic bridge decks due to its simplicity, speed, and theoretical grounding. in contrast, the morrice and little method remains an efficient, intuitive, and accessible tool, especially valuable for preliminary design, cross-checking, and situations where simplicity and speed are critical, but are limited in their accuracy when applied to complex geometries (Morrice and Little, 1954). While modern alternatives like Finite Element Method (FEM) offer advanced capabilities, they also introduce certain drawbacks which is often resource intensive and requires specialized expertise, making it less practical for preliminary design and routine assessment.Through the integration of these two complementary methodologies, the Hybrid Analytical Approach combines the rational, theory-based load distribution provided by the Morrice and Little design curves with the high geometric flexibility and detailed modelling capabilities of the Finite Element Method (FEM).

The use of a MATLAB-based matrix computation platform further enhances the efficiency of this approach. MATLAB's powerful matrix manipulation and programming allow for the development of an efficient computation that integrates both analytical and numerical models (Singh, 2006). These improved analytical capacities enable bridge engineers to better predict load effects and design to the best shape, resulting in enhanced safety, economy, and performance of orthotropic bridges today. In addition, this method can bridge the existing disparity between Indian and foreign codes by offering empirical recommendations as well as justified numerical procedures for skewed and curved decks subjected to related loadings. It also reduces reliance on expensive experimental studies and complex full 3D modeling by offering a balanced analytical-numerical solution (Argawal, Pal and Mehta, 2023).

CHAPTER TWO

2.0 LITERATURE REVIEW

Several studies have been carried out on Orthotropic Bridge deck, including elastic analysis of stiffened plates, buckling analysis of deck plate components, and strength evaluation of orthotropic deck and components. The combination of the Morrice and Little design curve method and finite element analysis (FEA) yields a hybrid analytical solution with the goal of improving the accuracy of orthotropic bridge deck analysis, particularly for skewed or curved geometry. The FEM uses similar stiffness-based methods, but rather than using beam elements with two nodes, it uses plate or shell elements with 3, 4 or more nodes. A key feature in FEM is in the mesh size, grillages whereas FEM models tend to need to be an order of magnitude smaller to achieve accuracy. With similar properties, spans and restraints the linear elastic FEM gives moments. This section will describe some aspects that are important to take in consideration when creating a FEM model. These will strongly affect the accuracy of results.

2.0.1 Element types

When applying FE software, it is important to choose an element type that is appropriate to describe the specific problem. There are three categories of elements that can be used in the analysis: structural elements, continuum elements and special elements. Structural elements resemble actual fabricated members such as cables, bars, beams and shells (Broo, 2008). Continuum elements are a decomposition of a continuum structure and can be used in two or three dimensions. Continuum elements have three degrees of freedom per node, which are all translations, while structural elements such as shells have six degrees of freedom which includes both rotations and translations (Austell, 2004). The last category is special elements which are used for modelling connections between

elements. Spring elements, contact elements and interface elements are examples of special elements (Broo, 2008).

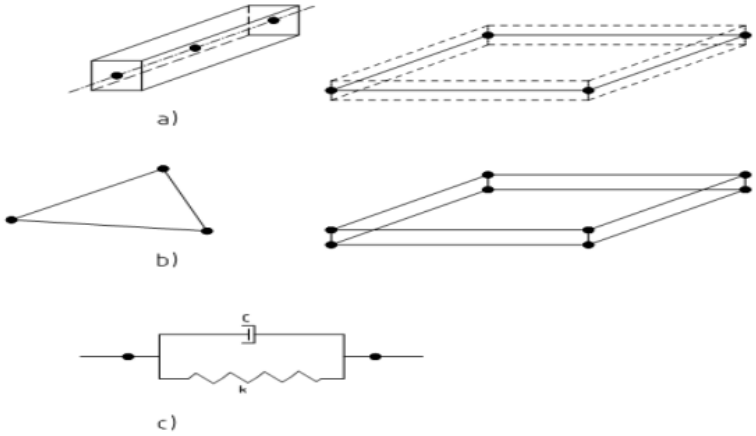

Figure 2.1: a) Structural elements e.g. beam elements and shell elements. b) Continuum elements in two or three dimensions. c) Special elements e.g. springs and dampers.

Some element types can have different accuracy depending on if results are interpolated linearly or with higher order between the nodes of the elements. The difference is what kind of shape functions that are used to describe the elements, linear or higher order (Ottosen, 1992). Figure 2.2 illustrates these different shape functions. By using higher order functions, the computation time can be reduced since the number of elements required to describe the structural behaviour may be less. But, if the same number of elements is used the computation time will increase since more complex shape functions are used.

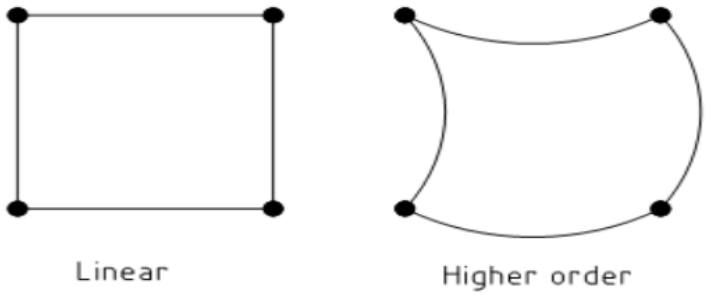

Figure 2.2: Difference between linear and higher order elements for a four-node element.

One way to reduce the running time is to use reduced numerical integration, which uses lower-order integration when establishing the stiffness matrix (Ellobody, 2014). The mass and load matrices are still integrated exactly. Figure 2.6 illustrates the difference between full and reduced integration.

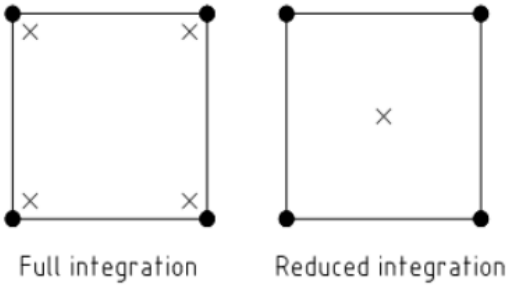

Figure 2.3: Difference between full and reduced integration.

2.0.2 Mesh sizing

The choice of mesh size is a very important aspect in the FE-analysis. The mesh should be chosen so that the result is sufficiently accurate with the shortest possible running time. To start with, the designer needs to define if the analysis should be carried out for the whole bridge or for individual bridge components. If the whole bridge is modelled with the exact geometry of each detail, the model will become very large and it might be impossible to run the analysis (Ellobody, 2014). One possibility is to create one main model that describes the global behaviour of the bridge and then local sub-models can be created to study the behaviour of individual details (Ellobody, 2014).

2.1 Orthotropic plate

In road bridges when roadway consists of road grid (longitudinal and transverse beams) and lying on her concrete slab, longitudinal and transverse beams are calculated as separate beams, independent of each other. The plate was seen also as a stand-alone bearing element independent of each other. Every part of the roadway performed only one function, without taking into consideration the relationship between the individual

parts. Some progress was made, when later reinforced concrete slab was joined by dowels to its supporting road grill. Thus, ensuring collaboration between the steel beams and reinforced concrete slab which with its effective width increased significantly the moment of inertia of the beam. However, plate already performed two functions took integral part of the road grid (like upper belt of longitudinal and transverse beams). The next decisive step taken were: a more accurate coverage of the forces exerted in the roadway, and to approach the actual work of the construction as the road began to be seen as a beam grid. Again, the plate was used as the upper belt of the beams. The calculation was conducted using a "rod statics" i.e. beam grid was seen as a system composed of individual bars (beams), without taking into account the spatial effect of the plate. In fact, but the roadway, consisting of orthogonally intersecting longitudinal and transverse beams, whose upper belts are connected to the deck plate, is forced to follow the deformations of the main girder and thus to work as an integral part of the main supporting system. Most decisive step in bringing and adapting the bridge construction to the actual distribution of actual distribution of internal effort, was made when determining the internal forces of the roadway was reduced to determining the internal forces of an orthogonal anisotropic plate i.e. when they were approached from bar to statics of continuum (continuous medium) (Cornelius, 1960). Resistance against bending of the roadway transverse plane to the axis of the bridge is much greater than resistivity its longitudinal axis. Upon this particular different elasticity of the roadway, in both cross and longitudinal direction, the explanation of the anisotropy of the plate followed.

2.2 Structural components of Orthotropic Bridge Deck

2.2.1 Wearing surface

The wearing surface on the OBD can be made from concrete, bitumen or polymer material (US Department of Transportation, 2012). The main purpose of the wearing

surface is to provide a skid resistant surface that gives a good ride quality. The wearing surface, however, also protects the deck from corrosion. The wheel pressure on the deck is often assumed to disperse at an angle of 45º in all directions through a bituminous layer. To be on the safe side, this dispersion is sometimes neglected, because it may be lost in higher temperatures when the wearing surface softens (US Department of Transportation, 2012

2.2.2 Deck plate

The deck plate of an OSD consists of a thin steel plate, which transfers the load to the ribs. As mentioned, the plate often acts as a common top flange for the stiffeners and for the main girders. The minimum thickness of the deck plate today is 14-16 mm; this is mainly due to the sensitivity to fatigue (US Department of Transportation, 2012).

2.2.3 Longitudinal stiffeners

Longitudinal stiffeners, also known as ribs, are mainly needed to provide supports for the slender deck plate. Two other functions of the longitudinal stiffeners are to increase the flexural rigidity of the cross section, and to help distribute the load to the transversal cross beams (US Department of Transportation, 2012). The most common practice is that they are continuous over the length of the deck, which means that cutouts need to be made in the cross beams. The ribs can be either open or closed, as seen in Figure 2.4.

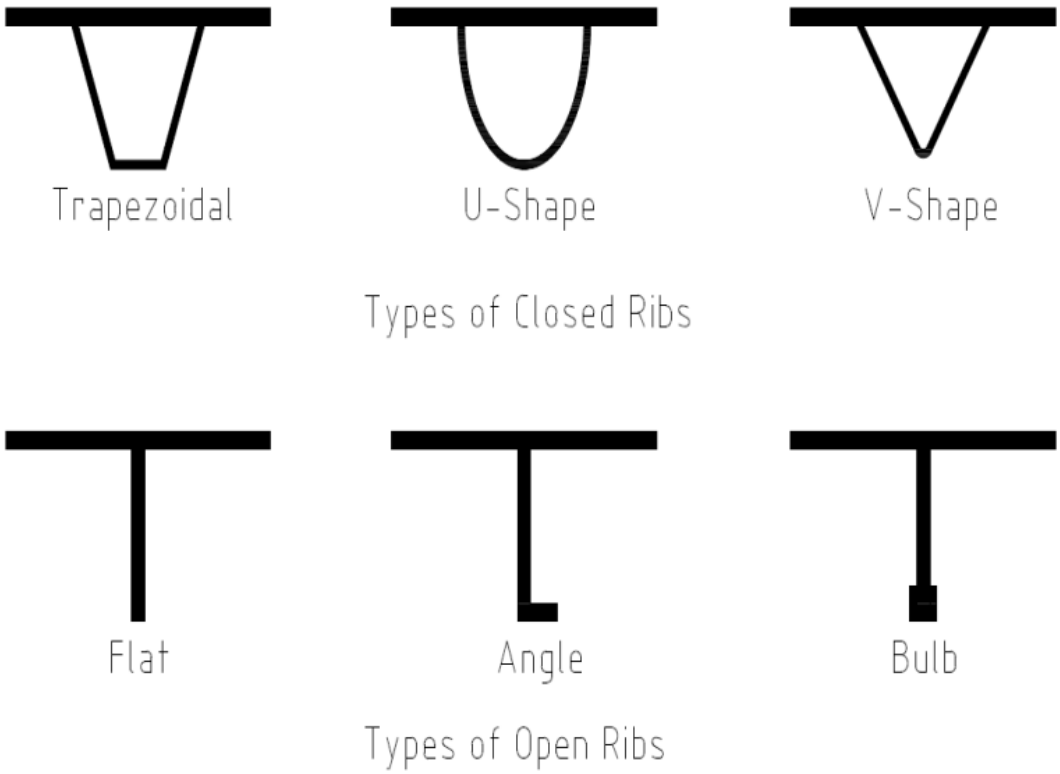

Figure 2.4: Closed and open Rid

The open ribs are simple to fabricate and are made from flat bars, bulb shapes, inverted T-sections, or angles (Figure 2.4) easily spliced in the field (AISC, 1963). They usually vary in size from 9mm by 203mm to 25mm by 305 mm (3/8 inch by 8 inches to 1 inch by 12 inches) along the cross-section of the bridge, and are spaced approximately 305 mm to 406 mm (12 inches to 16 inches) on center. Span lengths of open rib systems are generally in the range of 1.52 m to 3.05 m (5 to 10 ft).

They are also accessible for inspection and maintenance. Because of their simple geometry they provide a simpler analysis; therefore, they were popular in the pre computer era. The main disadvantage of the open longitudinal stiffeners is that they have essentially no torsional capacity (Mangus, 2000). The open ribs also have very little load distribution capacity in the transverse direction, which means that more longitudinal stiffeners are needed (AISC, 1963). Since no load is transferred transversally all load will go to the cross beams which then will be subjected to a greater load if the span is not

reduced, this means that the cross beams need to be spaced much closer. Thus, a solution with open ribs requires a great deal of material.

Experience indicates that it is simple to fabricate the open ribs and vary the rib dimensions as required for the various parts of the OSD. There are two main disadvantages of the open rib deck system. First, it is torsional soft relative to closed shapes. This means that it is not very efficient in distributing transverse loads such as wheels from one rib to adjacent ribs. This results in more ribs, closer FB spacing, and hence, more steel per square foot than a comparable closed rib system. Secondly, the total amount of welding required to fabricate the system is approximately double the amount required for a comparable closed rib system (i.e., a pair of vertical rib elements requires four lines of weld to the deck plate as opposed to two lines for a closed rib). Open ribs can be preferred in curved bridges due to ease of bending. Thus, economical designs may include some combination of open and closed ribs in the bridge cross-section.

The closed-rib system is the preferred system relative to open-ribs for a number of reasons. First, the closed ribs are advantageous to use because of their high flexural and torsional rigidity (AISC, 1963). The high torsional rigidity contributes to better distribution of concentrated transverse loads and, consequently, to a reduction in stresses in the deck plating. Fewer welds, less distortion, and reduced steel weight are further advantages. They also possess a good load distribution capacity in the transverse direction, which in turn means that fewer longitudinal stiffeners are needed, and the spacing between the transversal cross beams can be longer. This also reduces the dead weight of the structure. Another advantage with closed ribs is that there is less surface area that needs to be protected against corrosion, then in a system with open stiffeners (Mangus, 2000). The main disadvantages of the closed ribs are that they are more

difficult to fabricate and that the deck becomes more complex to analyse because of more interaction between the parts of the deck (AISC, 1963).

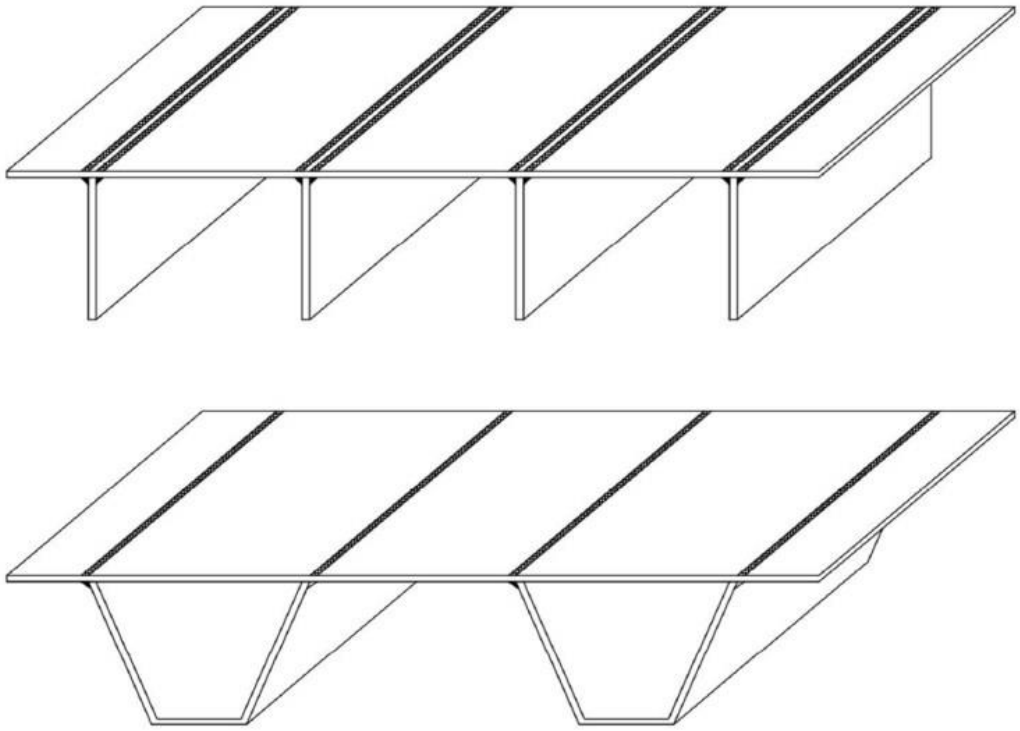

Figure 2.5: Amount of welding required in open and closed ribs (Karlsson, 2015).

The most commonly used stiffener today is the closed trapezoidal rib (Kolstein, 2007). This type of stiffener gives the highest torsional rigidity. The U-shaped rib has a rounded bottom which gives lower stress concentration, but the torsional rigidity of this rib type is much less than that of the trapezoidal ribs (AISC, 1963). Open ribs are still sometimes used to stiffen box girder webs and bottom flanges (US Department of Transportation, 2012). They can also be used in curved bridges, where it is difficult to use closed ribs. The current trend is to use longer spans of the longitudinal stiffeners (US Department of Transportation, 2012).

However, this means that the stiffeners need to be higher, which leads to larger cut-outs in the web of the transversal stiffeners. This can lead to problems with the shear capacity of the transversal stiffener.

2.2.4 Transversal stiffeners

The transversal stiffener, also called cross beam or floor beam, is normally an inverted T-section, which is welded to the deck plate (AISC, 1963). As mentioned before, the plate acts as a top flange for the cross beam.

The main functions of the cross beam are to transfer the load transversally to the main girders and to provide support to the ribs (US Department of Transportation, 2012). In the cross beam there are often cut-outs for the longitudinal stiffeners. These are often made larger than the ribs in order to reduce the stress concentration at the intersection (US Department of Transportation, 2012). These cut-outs, however, have a substantial impact on the moment and shear capacity of the cross beam, which must be taken into account.

2.3 Orthotropic Plate Theory

Orthotropic Plate Theory is an extension of classical Deck theory designed to model plates whose mechanical properties differ along different orthogonal directions. It is widely used in structural engineering, particularly for analysing bridge decks, ship hulls, aircraft panels, and composite materials, where materials exhibit direction-dependent behaviour.

An orthotropic Deck is a structural element where the stiffness and strength vary along two or three mutually perpendicular directions (typically, the longitudinal, transverse, and through-thickness directions). This behaviour contrasts with isotropic plates, where properties are identical in all directions.

In most practical cases:

i Two-way orthotropy refers to differing properties along two in-plane directions (e.g., x and y axes).

ii Examples include steel bridge decks with stiffeners, Fiber-reinforced composite plates, and laminated materials.

The analysis of an isotropic plate was first presented by Gehiring (1860) and Boussinesq (1879). The complete solution for isotropic plate was presented by Huber (1914). The differential equation giving the relationship between the lateral deflection and the loading of an orthotropic deck, Equation (1.1), is referred as Huber's equation. The bending behaviour of an orthotropic Deck is described by a modified version of the classic plate equilibrium equation:

$$Dx\frac{\partial^4\omega}{\partial x^4} + 2D_{xy}\frac{\partial^4\omega}{\partial x^2\,\partial y^2} + D_y\frac{\partial^4\omega}{\partial y^4} = (x, y) \quad (2.1)$$

Where:

(x, y) = transverse displacement of the plate.

q (x, y) = distributed transverse load.

$D_{x,y}$ = flexural rigidities along the x and y directions.

D_{xy} = coupling rigidity (due to Poisson effects and orthotropy).

Flexural rigidities are defined as:

$$D_x = \frac{E_x h^3}{12(1 - v_{xy}v_{yx})} \quad (2.2)$$

$$D_y = \frac{E_y h^3}{12(1 - v_{xy}v_{yx})} \quad (2.3)$$

$$D_{xy} = \frac{G_{xy}h^3}{12} \quad (2.4)$$

Where:

$E_{x,y}$ = Young's moduli in the x and y directions.

$v_{xy,yx}$ = Poisson's ratios

G_{xy} = in-plane shear modulus.

h = plate thickness.

The basic assumption proposed by Huber for estimating the overall bending deflections and bending stresses in a stiffened plate, is to replace it by an equivalent orthotropic Deck of constant thickness having the same orthogonal stiffness characteristics. This is called the Method of Elastic Equivalence (MEE). Guyon (1946) used the method to analyze a deck without torsional stiffness of the rib. Massonnet (1950) extended the method to include the torsional stiffness. This work was further developed by Morice, Little and Rowe (1956). Rowe (1962) summarized the design technique based on a series solution of the governing partial differential equation at a stage before the widespread availability of the electronic digital computer. In 1946 Yves Guyon introduced his theory of a zero-torsion grillage, which was grounded on Huber's orthotropic plate theory (Guyon, 1946). Massonnet in 1949 expanded Guyon's, i.e. at the same time coinciding with the development of grillage theories of Leonhardt/Andrä and Homberg. Massonnet devised graphs for simply supported beams, constant moment of inertia and identical moment of inertia for all main girders. He therefore, created another method for the simple analysis of grillages. Between 1955 and 1960 (Sattler 1974), further refined these graphs to cover main girders with a varying moment of inertia, perimeter and inner beams with different moments of inertia and any structural system (Kurrer 2011). Finally, in 1966, the monograph of (Bareš and Massonnet) appeared, which embraced all the findings based on the Guyon/Massonnet method and delivered a series of new ideas, experience and practical insights.

Orthotropic Deck Theory represents a crucial advancement in structural analysis, bridging the gap between simplistic isotropic models and the complex real-world behavior of stiffened, composite, and directionally dependent plate structures.

2.3.1 The theory of Guyon and Massonnet

In 1946 that Yves Guyon introduced his theory of a zero-torsion grillage based on Huber's orthotropic plate theory (Guyon, 1946). Massonnet in 1949 expanded upon Guyon's work, i.e. Coinciding with the development of grillage theories of Leonhardt/Andrä and Homberg. Massonnet devised graphs for simply supported beams, constant moment of inertia and identical moment of inertia for all main girders. He therefore provided a simplified approach for analysis of grillages. Over the years 1955-1960 (Sattler 1974), extended the graphs to cover main girders with a varying moment of inertia, perimeter and inner beams with difference between moments of inertia, perimeter and interior beams and any structural system. (Kurrer, 2011). Finally, in 1966, the monograph of (Bareš and Massonnet) appeared, which embraced all the findings based on the Guyon/Massonnet method and delivered a series of new ideas and experience.

2.4 Morrice and Little Design Curve Method in Bridge Deck Analysis

The Morrice and Little method is a classical design aid that employs distribution coefficients or design curves to simplify complex bridge deck load distributions into equivalent systems with uniform loading (Chhandak Biswas, 2025). The method is also based on the principle that the load share of the girder is related to the relative deflection the girder under load.

It provides arithmetical coefficients (distribution factor K) approximating the manner in which loads distribute across orthotropic or composite decks, which allows for quick and practical design calculations. The deck is treated as a grillage and a much stricter analysis is made of the deflecting behavior of the deck in the transverse direction. For that purpose, the deck is divided into eight equal parts and its flexural capacity and torsional capacity is computed in terms of two parameters θ and α respectively. Division of the deck into eight equal parts results in nine boundary points. The

deflections under each of these points need to be considered with loads placed also at each. Morice-Little curves have been evolved to provide the arithmetical coefficient known as distribution coefficient K for such deflection. Actual deflection of the deck at the boundary point under proposed load will be K times average deflection of the deck that will take place when the load is uniformly distributed across the deck. Since deflection at any location is directly related to the bending moments, they can be applied to arrive at the longitudinal bending stresses also.

Morice–Little curves comprise 12 sets of curves. Six of them for deck with no torsional stiffness $\alpha = 0$ (designated for convenience as K_0) and six curves for deck with maximum torsional stiffness $\alpha = 1$ (designated as K_1). The distribution coefficient for a deck with torsional stiffness parameter α for a bridge deck is arrived at by applying the equation:

$$Ka = K_0 + (K_1 - K_0)\sqrt{a} \tag{2.5}$$

Since there has been some approximation in arriving at these curves, a correction factor of 10% is applied to the bending moments and stresses arrived at using these graphs to represent the actuals under concentrated loads (Victor's book[2]). This method is quite appropriate for early design stages and for bridges having simple geometries; however, its application is cumbersome with curved or skewed bridges due to geometric complexity (Kirkpatrick James, 1982).

2.5 Finite element method for Orthotropic Bridge Decks

Finite Element Method for orthotropic bridge decks thrives when global homogeneity and local detail are both captured homogenized plates for system-level behavior complemented by detailed sub models for fatigue critical zones. Finite element procedures provide a general numerical tool to model the detailed structural behavior of Orthotropic bridge decks, including complexities like skewness, curvature, and anisotropic material behavior. With validation from experiments, FEM becomes a

powerful tool to design lighter, more durable bridges with controlled maintenance demands. FEA allows for a close mesh modeling and accounts for realistic boundary conditions in order to investigate stresses, deflection, and dynamic responses that are difficult to estimate by the use of simpler methods alone. Finite Element Method addresses static, dynamic and time dependent challenges. Advances in software and modeling techniques continues to enhance efficiency, though challenges like weld modelling and corrosion effects require ongoing research. Research has particularly highlighted the effectiveness of FEA for the modeling of skewed and curved decks where traditional analytical methods are insufficient (Powell and Ogden, 1969). FEM remains a cornerstone for modern bridge engineering.

2.6 Finite element modelling

FEM uses shell element with orthotropic properties to represent the deck, providing adequate details for directional stiffness. For example, slab can be modelled as equivalent solid plates, simplifying analysis while maintaining accuracy. Software tools automate this process. The FE model is established by creating different parts that are assembled together to form the bridge model.

All parts are connected with the assumption that they are perfectly fixed to each other. The FE model of the bridge is illustrated in Figure 2.6 The marked section of the bridge is where the loads are placed.

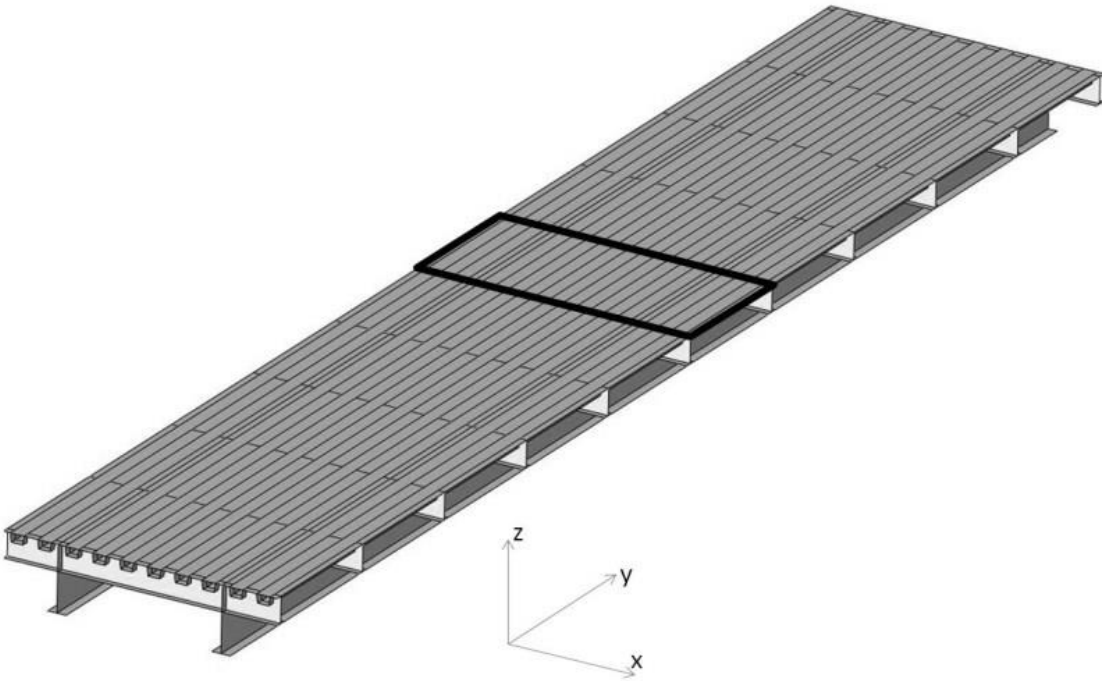

Figure 2.6: Bridge geometry in FE-model.

The marked section is where the wheel loads are placed. All parts are assigned isotropic material properties, for the detailed shell model, with Young's modulus 210 GPa and Poisson's ratio 0.3. All analyses performed are linear elastic which means that yielding and other non-linear effects are not of interest. Therefore, no other material parameters are needed to describe the material.

2.7 Finite Element Modelling Techniques

FEM involves disintegrating the structure into smaller elements example: shell or bar element (section 2.0.1) and solving for the structural response under subjected loads. For Orthotropic Bridge Decks, the following modelling approaches are popularly used:

i Orthotropic plate theory (section 2.3): As further explained in (section 2.3) this theory treats the deck as an equivalent solid plate with orthotropic material properties, where stiffness differs in longitudinal and transversal direction. This approach is majorly efficient for concrete decks with voids, as it accounts for the deformable nature of the cross section.

ii Equivalent orthotropic material modelling (EOMM): For complex decks with multiple stiffeners, EOMM simplifies the model by representing the deck as equivalent shell element with orthotropic properties. This method matches the longitudinal, lateral and shear stiffness of the original configuration, making it suitable for analysing multi-scale dynamic loads, such as vehicle-imposed impacts. A case study as described in (section 1.4) short span bridge 4m length, 2.45m width.

iii Element types and connections (section 2.0.1 and 2.1.2): typical FEM models include; orthotropic shell elements for the deck, Bar elements for modelling post tensioning cables or reinforcement, rigid elements for force transmission between components.

The choice of element type and mesh density is crucial, with finer meshes required around stress concentration areas like welds to capture local behaviours accurately (section 2.0.1 and 2.1.2).

2.8 Integration of Morrice and Little with Finite Element Analysis

Ongoing research aims at merging the design curves of the Morrice and Little method with finite element frameworks to create a hybrid methodology that couples empirical design experience with numerical accuracy.

The hybrid methodology employs distribution coefficients to approximate load distribution while FEA improves response modeling for complex geometrical and loading conditions. The outcome is a balanced methodology that is computationally efficient but accurate for curved and skewed orthotropic bridge decks (Kanwarjot Singh, (n.d.) pdf). Using both yields a robust, efficient hybrid workflow: Morrice and Little for speed and initial design; FEM for accuracy and validation.

2.9 Role of MATLAB and Matrix Computation Techniques

MATLAB, as a high-level matrix computation language, has been an indispensable tool in the execution of the hybrid analytical procedure. Matrix representations enable efficient computation of load distributions, system responses, and stiffness matrices in finite element modeling of the orthotropic bridge decks and T-girder. The integration of Morrice and Little's coefficients in MATLAB-based FEA models facilitates an integrated workflow that incorporates design curve inputs and extensive numerical analyses. The approach also facilitates parametric and sensitivity studies, whereby engineers can examine different skew angles and geometrical layouts with enhanced accuracy (Farhan and Dewangan, 2022).

2.10 Accuracy and Practical Benefits

Comparative studies demonstrate that the hybrid approach yields results of higher accuracy than purely empirical or purely numerical methods individually. It reduces discrepancies in load distribution factors and better predicts structural behavior for various load cases, especially in skewed or curved decks where traditional analytical solutions are less reliable. Computer software such as CSiBridge incorporates aspects of this hybrid method, enabling practical engineering applications (Rafizadeh and Gharighoran, 2019).

2.11 Conclusion of Literature Review

The reviewed literature emphasizes the importance of the synthesis of Morrice and Little design curves and finite element analysis aided by MATLAB matrix computations give a robust method for orthotropic bridge deck analysis with particular reference to skew and curved complexities. The hybrid approach combines the computational efficiency of the design method and the detailed modeling ability of FEA for enhanced accuracy, computational efficiency, and practicality in modern bridge engineering.

CHAPTER THREE

METHODOLOGY

3.1 Study Area

This research focuses on the structural analysis and design optimization of skewed or curved orthotropic bridge decks. Although the primary analysis is conducted through computational methods rather than physical experimentation, this study considers a hypothetical or representative bridge deck segment as the model case. The study area encompasses potential bridge types with skewed geometries, typically found in highway and railway infrastructure, characterized by specific geometric and material properties. For the purposes of this analysis, the bridge deck is modeled with a typical orthotropic steel deck, incorporating anisotropic elastic properties pertinent to the material and geometric configuration (Soban et al., 2021). Relevant diagrams illustrating the deck geometry, including the skew angle and curvature parameters, are utilized to define boundary conditions and loading scenarios.

3.1.1 Bridge geometry

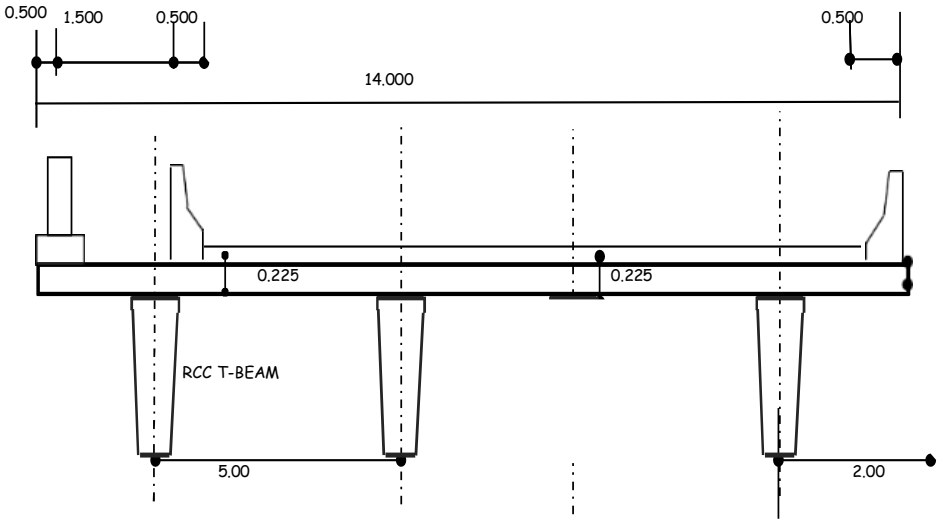

Figure 3.1: The cross-section of the composite bridge deck.

The deck slab was analysed in the transverse direction as a continuous slab system supported on longitudinal girders, with cantilever overhangs on both sides. To simplify the analysis while capturing the essential behaviour, a unit-width strip of the deck was considered along the span, a common approach in orthotropic deck design. This allowed for detailed evaluation of transverse bending and shear behaviour under various loading conditions. The structural analysis considered multiple loading types in compliance with relevant design codes: Dead Load (DL), Superimposed Dead Load (SIDL), Footpath Live Load (FPLL), and Carriageway Live Load (CWLL). These loads were applied to simulate real-world service conditions. Additionally, to capture the effect of load transfer and rotational restraint at supports, equivalent forces and moments were applied at the ends of the slab strip, representing boundary effects from adjacent structural elements.

The entire transverse analysis was conducted using STAADPro v8i, which enabled precise modelling of slab geometry, boundary conditions, and loading configurations.

3.2 Procedures and Methods of Analysis

The methodology involves a hybrid approach that integrates the Morrice and Little (Design Curve) method with finite element analysis (FEA) to produce a comprehensive understanding of the bridge deck behavior under various loading conditions.

3.2.1 The Morrice and Little Design Curve Method

The Morrice and Little method involves the use of empirically derived design curves that relate the load-bearing capacity of orthotropic bridge decks to their geometric and material properties. This approach simplifies preliminary design calculations by providing reference values for flexural strength, shear capacity, and other critical parameters based on standard configurations (Morrice and Little, 1964).

i. The design curve data are obtained from the standard charts provided in Morrice and Little's literature, which relate parameters such as deck span, thickness, and skew angle to permissible load levels.

ii. The appropriate design curves are selected based on the deck geometry and specified material properties.

iii. Load capacity and stress limits are estimated through interpolation directly from the curves, providing initial design benchmarks.

3.2.2 Finite Element Modeling in MATLAB

To refine and validate the initial design assumptions, a finite element model of the orthotropic bridge deck is constructed using MATLAB, leveraging its matrix computation capabilities.

3.2.2.1 Model Development

i. The deck is discretized into a mesh of two-dimensional finite elements, typically using shell or plate elements suitable for orthotropic material properties.

ii. The element stiffness matrices are derived considering anisotropic elasticity, incorporating elastic moduli, Poisson’s ratios, and shear moduli relevant to steel orthotropic decks (Timoshenko and Woinowsky-Krieger, 1959).

3.2.2.2 Incorporation of Material Anisotropy

i. The orthotropic material behavior is integrated within the stiffness matrix formulation by defining separate elastic constants for longitudinal, transverse, and shear directions.

ii. MATLAB matrices are employed to assemble the global stiffness matrix (K), applying boundary conditions to simulate supports and loadings consistent with actual bridge configurations.

3.2.2.3 Loading and Boundary Conditions

i. Vertical loads simulating traffic or environmental effects are applied uniformly or selectively across the mesh nodes.

ii. Boundary conditions represent simply supported or fixed edges, consistent with typical bridge supports.

3.2.2.4 Analysis and Solution

i. The software solves the system of equations $K \times \delta = FK \times \delta = F$ where $\delta\delta$ is the displacement vector and FF is the load vector.

ii. Stress and strain distributions are computed from nodal displacements, considering the orthotropic material stiffness matrix.

3.2.2.5 Validation and Comparison

i. Results from the finite element analysis are compared with the initial estimates obtained from the Morrice and Little design curves.

ii. Discrepancies are analyzed to identify the effects of skewness and curvature not captured by the empirical method.

3.3 Integration of Methods

The hybrid approach involves iterative feedback:

i. The Morrice and Little method provides a quick and conservative estimate of the deck's capacity, guiding initial design parameters.

ii. The MATLAB-based FEA offers detailed stress-strain analysis, capturing effects of skewness and curvature that empirical curves may oversimplify.

iii. Adjustments are made to the design parameters based on FEA results, enhancing accuracy and safety margins.

3.4 Implementation in MATLAB

The programs developed for this hybrid analysis utilize MATLAB's matrix operations for efficient computation. The following steps describe the code implementation:

3.4.1 Mesh Generation

i. MATLAB scripts generate the finite element mesh based on input dimensions.

3.4.2 Material Property Definition

i. Input parameters for orthotropic elastic constants are defined as matrices.

3.4.3 Stiffness Matrix Assembly

i. Element stiffness matrices are assembled into the global stiffness matrix using MATLAB's sparse matrix capabilities.

3.4.4 Applying Loads and Boundary Conditions

i. Boundary constraints and load vectors are constructed with MATLAB matrices.

3.4.5 Solution

i. MATLAB's linear algebra solver computes displacements, stresses, and strains.

3.4.6 post-processing

i. Results are visualized and compared against the empirical design estimates.

3.5 Orthotropic Bridge Deck Loading

3.5.1 HA Loading

According to the Design Manual for Roads and Bridges (BD 37/01), Type HA loading is the standard design loading for Great Britain and sufficiently accounts for the impacts of all conventional vehicles that are allowed, with the exception of those used for abnormal indivisible loads. The Road Vehicles (Authorized Weight) Regulations 1998, often known as the AW Vehicles, regulate normal vehicles and apply to those weighing up to 44 tons gross vehicle weight. These AW vehicles' loads are shown as a knife-edge load

and an evenly dispersed load. The loading has been increased to include impact load, which is what happens when wheels "bounce," or when potholes are struck. over-loading

Lateral bunching is when multiple cars take up a lane's width.

For the member in question, the loaded length as established by the influence line determines the size of the uniformly distributed load. In the case of merely supported decks, this typically pertains to the deck's span. The fundamental applied load, known as 9HA loading, is made up of two parts: an evenly distributed load and a knife-edge load. HA loading accounts for impact by 25%.

Its intensity is determined by the length of load

No load distribution below the contact area

The position of the knife-edge load is intended to have the most detrimental impact.

Table 3.1: Notional Lanes for design purposes according to the carriageway width

Carriage Width (m)	5 –7.5	7.5 –10.95	10.95 –14.6	14.6 – 18.25	18.25 - 21.9
No. of Notional	2	3	4	5	6

Source: (BD 37/0)

Table 3.2: HA Loading

Loaded length L (m)	< 50 m	50 m - 1600 m	> 1600 m
Uniform Load (kN/m/Lane)	$336(1/L)^{0.67}$	$36(1/L)^{0.1}$	Agreement
Knife edge (kN/Lane)	120KN		

Source: (BD 37/0)

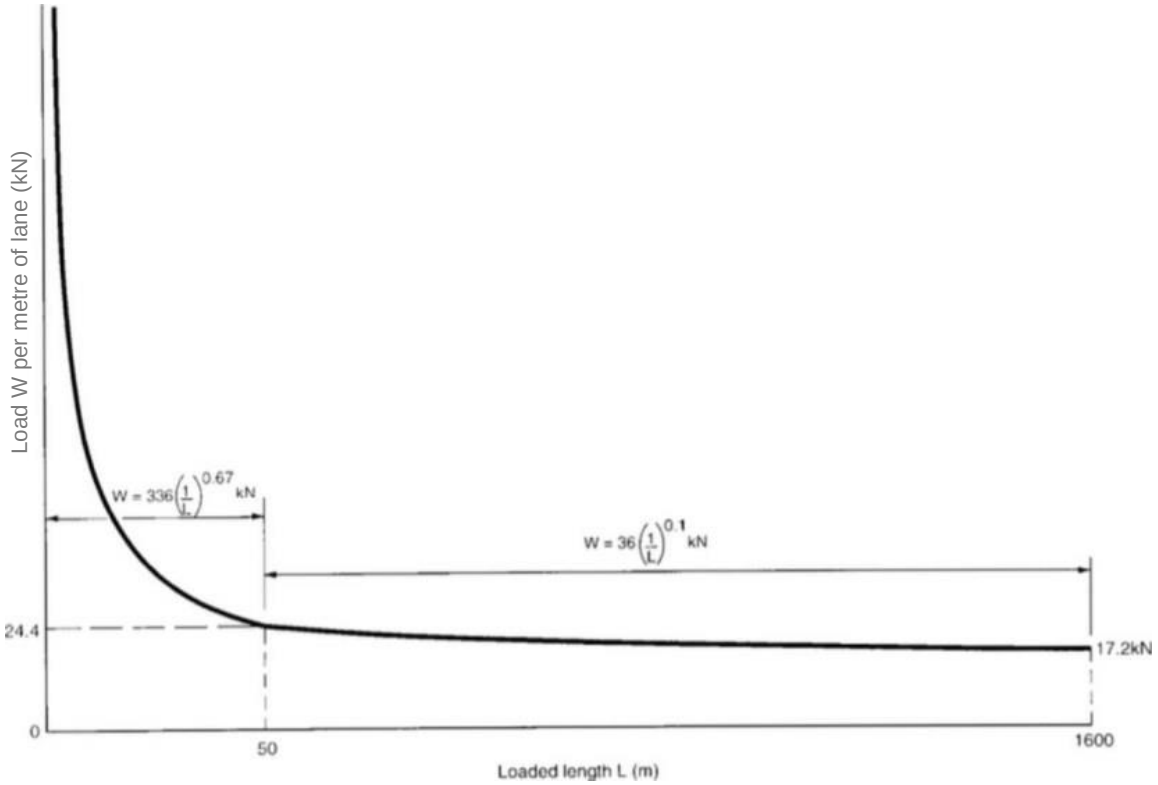

Figure 3.2: Loading curve HA UDL (Not to scale)

3.5.1.1 HA Factors Lane

Table 3.3: HA lane factors

Loaded length L m	**First lane factor β_1**	**Second lane factor β_2**	**Third lane factor β_3**	**Fourth and subsequent β_n**
0 < L ≤ 20	α1	«1	0.6	0.6 α1
20 < L ≤ 40	α2	«2	0.6	0.6 α2
40 < L ≤ 50	1.0	1.0	0.6	0.6
50 <L ≤ 112 N<6	1.0	7.1 / L	0.6	0.6
50 <L ≤ 112 N≥ 6	1.0	1.0	0.6	0.6
L>112 N<6	1.0	0.67	0.6	0.6
L>112 N ≥ 6	1.0	1.0	0.6	0.6

NOTE $\alpha 1 = 0.274\ b_L$ and cannot exceed 1.0

$\alpha 2 = 0.0137\{b_L(40 - 1) + 3.65(1 - 20)\}$

where b_L is rhe notional lane width (m)

NOTE: N shall be used to determine which set of HA lane factors is to be applied for loaded lengths in excess of 50m. The value of N shall be taken as the total number of notional lanes on the bridge this shall include all the lanes for dual carriageway roads) except that for a bridge carrying one-way traffic only, the value of A' shall be taken as twice the number of notional lanes on the bridge.

Source: (BD 37/0)

3.5.2 HB Loading

Type HB loading criteria are based on the characteristics of extraordinary industrial loads (such as electrical transformers, generators, pressure vessels, machine presses, etc.) that are expected to utilize the local roadways, according to the UK's (BD 37/0) Design Manual for roadways and Bridges. A vehicle with four wheels evenly spaced on each axle serves as a representation of the vehicle load. The number of units that determine the load on each axle depends on the type of route. 45 units are needed for motorways and trunk roads, 37.5 units are needed for principal routes, and 30 units are needed for minor public roads. 10kN is equal to each unit. Bridges on public roadways that might experience abnormal loads higher than those resulting by HA loading are susceptible to HB loading. It specifies a 16-wheel vehicle. 2.5 j kN is the load/wheel, where j is the number of HB units. There is a range of 25 to 45 HB units for the HB loading. For example, a truck with 25 units x 2.5 x 16 wheels would weigh 1000 kN, or 100 tons. A truck with 45 units x 2.5 x 16 wheels weighs 1800 kN, or 180 tons. The relevant government in each nation often specifies the actual units to be used for a given bridge. Additionally, HB loading incorporates a 25% impact allowance.

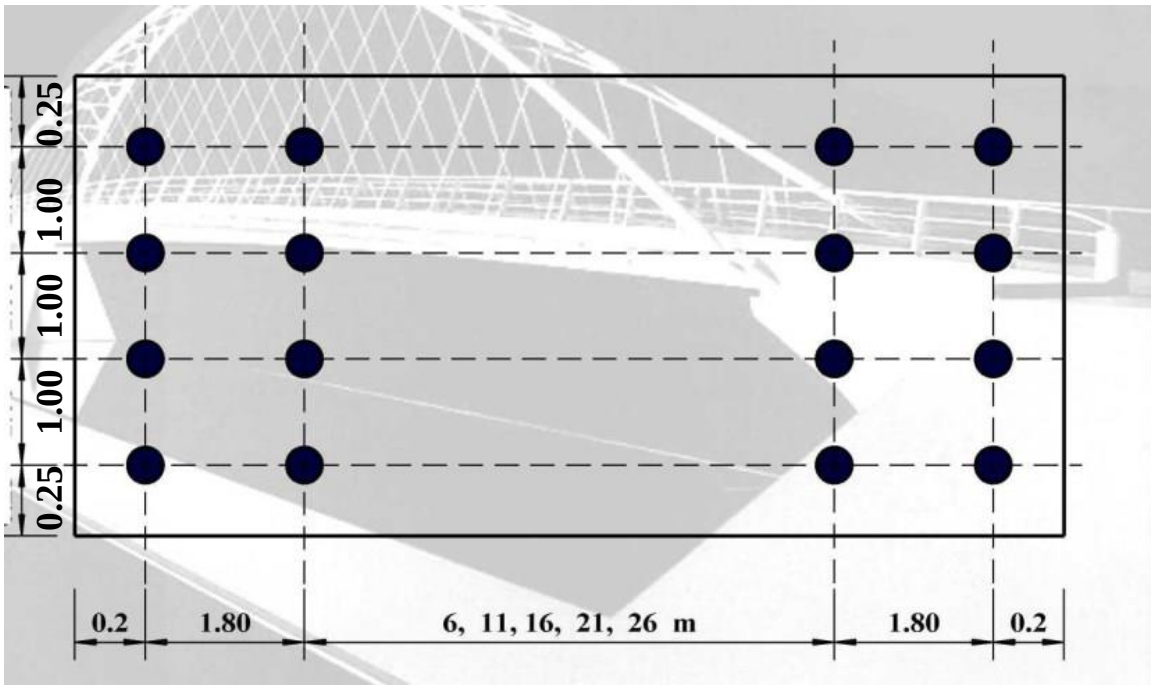

Figure 3.3: HB Vehicle (BD 37/0)

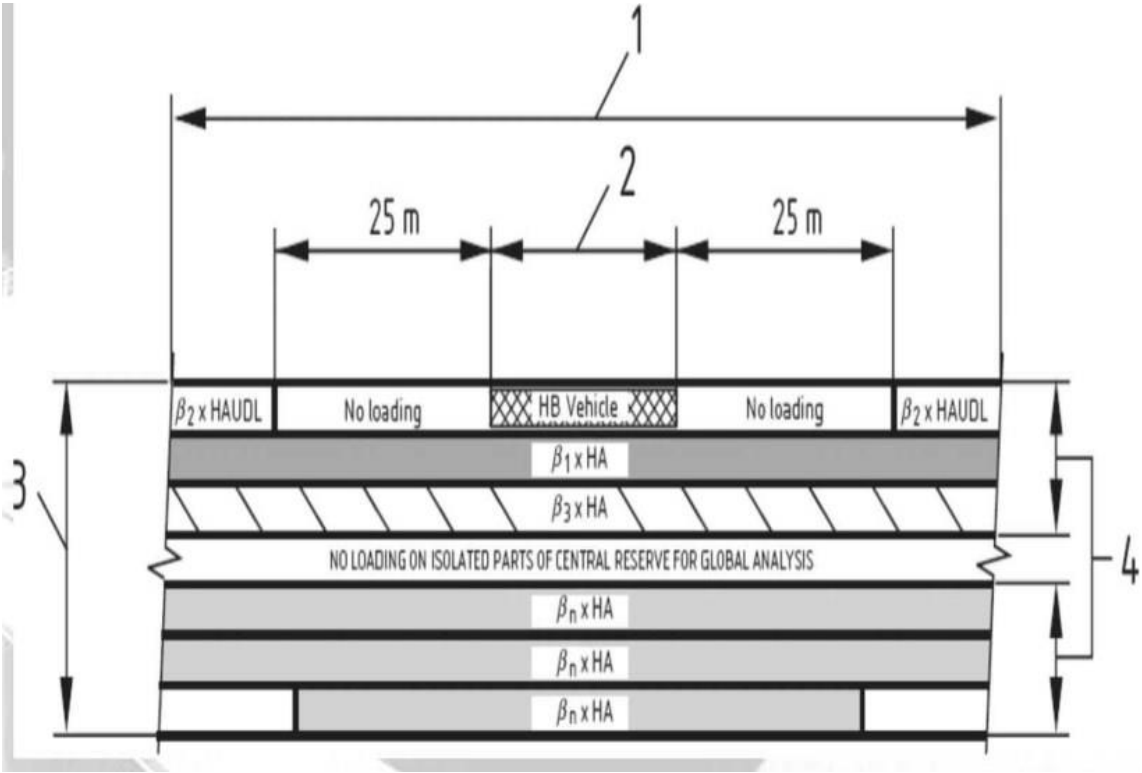

Figure 3.4: A combination of HA and HB loading: HB within one notional lane (BD 37/0)

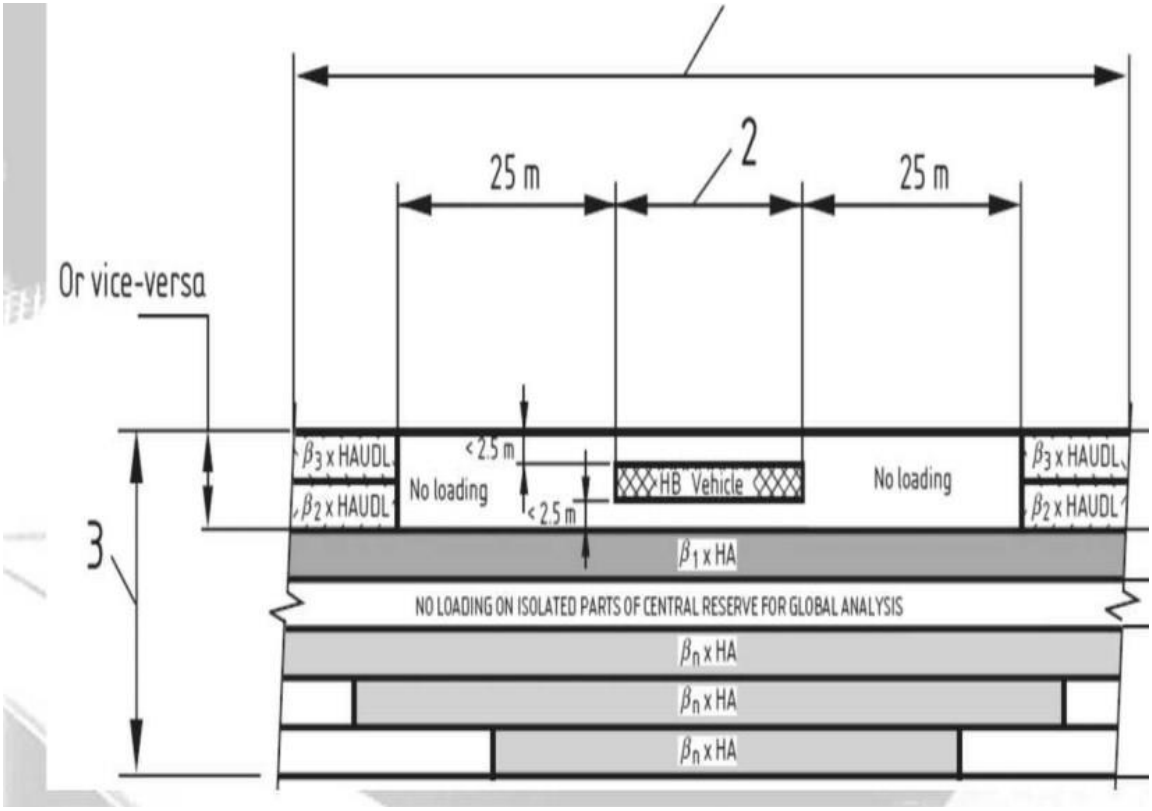

Figure 3.5: A combination of HA and HB loading; HB occupying two notional lanes (BD 37/0)

CHAPTER FOUR

RESULTS AND DISCUSSION

4.1 Introduction

This chapter presents the results obtained from the hybrid analytical framework developed in MATLAB, integrating the Morrice and Little (Design Curve) method with the Finite Element Method (FEM). The results focus on orthotropic bridge deck (OBD) models subjected to HA and HB loadings. The chapter discusses numerical findings, compares Morrice and Little estimates with FEM outcomes, and evaluates the effectiveness of the hybrid method in improving accuracy and efficiency in bridge deck analysis.

4.2 Results from Finite Element Analysis (STAAD pro Design)

The finite element analysis (FEA) conducted using STAADPro v8i provided a comprehensive understanding of the structural performance of the orthotropic bridge deck (OBD) under BS 5400 HA and HB loadings. The model incorporated 3 main longitudinal girders (W900 × 300 mm), 200 × 12 mm longitudinal ribs spaced at 300 mm, and cross-girders at 2 m intervals, forming a typical orthotropic deck layout. The deck spanned 30 meters and was simply supported at both ends, with a total width of 14 metres, simulating a real-world highway bridge configuration. Table 4.1 shows the sectional properties of key structural components used in the STAADPro finite element model. Table 4.2 presents the plate thickness assignments at different nodal points (A, B, C, D) of the orthotropic deck model. Table 4.3 defines the material properties used in the finite element analysis.

Table 4.1: Section Properties

Prop	Section	Area (cm^2)	I_{yy} (cm^4)	I_{zz} (cm^4)	J (cm^4)	Material
2	CB40X102	6.072	353E+6	24E+9	0.000	STEEL
3	WRF	319.800	48.4E+3	209E+3	796.104	STEEL

Source: Staad Pro v8i Design Sheet

Table 4.2: Plate Thickness

Prop	Node A (cm)	Node B (cm)	Node C (cm)	Node D (cm)	Material
1	20.000	20.000	20.000	20.000	STEEL

Source: Staad Pro v8i Design Sheet

Table 4.3: Material Properties

Mat	Name	E (kN/mm^2)	v	Density (kg/m^3)	α (/°C)
1	Steel	205.000	0.300	7.83E+3	12E -6
2	Stainless Steel	197.930	0.300	7.83E+3	18E -6
3	Aluminum	68.948	0.330	2.71E+3	23E -6
4	Concrete	21.718	0.170	2.4E+3	10E -6

Source: Staad Pro v8i Design Sheet

Table 4.4: Primary Load Cases

Number	Name	Type
1	Dead Load Case 1	Dead
2	BS5400: SLS BS5400_Gen_Load N39: Disp	Live
3	BS5400: SLS BS5400_Gen_Load N33: Reac	Live
4	BS5400: SLS BS5400_Gen_Load N34: Reac	Live
5	BS5400: SLS BS5400_Gen_Load N35: Reac	Live
6	BS5400: SLS BS5400_Gen_Load N36: Reac	Live
7	BS5400: SLS BS5400_Gen_Load N37: Reac	Live
8	BS5400: SLS BS5400_Gen_Load N38: Reac	Live
9	BS5400: SLS BS5400_Gen_Load N39: Disp	Live
10	BS5400: SLS BS5400_Gen_Load N33: Reac	Live
11	BS5400: SLS BS5400_Gen_Load N34: Reac	Live
12	BS5400: SLS BS5400_Gen_Load N35: Reac	Live
13	BS5400: SLS BS5400_Gen_Load N36: Reac	Live
14	BS5400: SLS BS5400_Gen_Load N37: Reac	Live
15	BS5400: SLS BS5400_Gen_Load N38: Reac	Live
16	BS5400: SLS BS5400_Gen_Load N39: Disp	Live
17	BS5400: SLS BS5400_Gen_Load N33: Disp	Live
18	BS5400: SLS BS5400_Gen_Load N34: Disp	Live
19	BS5400: SLS BS5400_Gen_Load N35: Disp	Live
20	BS5400: SLS BS5400_Gen_Load N36: Disp	Live
21	BS5400: SLS BS5400_Gen_Load N37: Disp	Live
22	BS5400: SLS BS5400_Gen_Load N38: Disp	Live
23	BS5400: SLS BS5400_Gen_Load N1: Disp Y	Live
24	BS5400: SLS BS5400_Gen_Load N5: Disp Y	Live
25	BS5400: SLS BS5400_Gen_Load N9: Disp Y	Live
26	BS5400: SLS BS5400_Gen_Load N25: Disp	Live
27	BS5400: SLS BS5400_Gen_Load N33: Disp	Live
28	BS5400: SLS BS5400_Gen_Load N39: Disp	Live
29	BS5400: SLS BS5400_Gen_Load N40: Disp	Live
30	BS5400: SLS BS5400_Gen_Load N41: Disp	Live
31	BS5400: SLS BS5400_Gen_Load N33: Reac	Live
32	BS5400: SLS BS5400_Gen_Load N34: Reac	Live
33	BS5400: SLS BS5400_Gen_Load N39: Disp	Live
34	BS5400: SLS BS5400_Gen_Load N33: Reac	Live

Source: Staad Pro v8i Design Sheet

Table 4.5: BS5400: SLS BS5400_Gen_Load N39: Disp Y -ve: Plate Loads

Plate	Type	Direction	F_a	X1 (m)	Y1 (m)	X2 (m)	Y2 (m)
26	PRE N/mm^2	G_Y	-7.160	-5.125	-1.469	-4.515	-1.059
	PRE N/mm^2	G_Y	-7.160	-3.065	-1.469	-2.455	-1.059
	CON kN	G_Y	-10.240	-5.125	-6.949	-4.515	-6.539
	CON kN	G_Y	-10.240	-5.125	-5.429	-4.515	-5.019
	CON kN	G_Y	-10.240	-3.065	-6.949	-2.455	-6.539
	CON kN	G_Y	-10.240	-3.065	-5.429	-2.455	-5.019
	CON kN	G_Y	-10.340	-5.125	-14.869	-4.515	-14.459
	CON kN	G_Y	-10.340	-5.125	-13.499	-4.515	-13.089
	CON kN	G_Y	-10.340	-5.125	-10.449	-4.515	-10.039
	CON kN	G_Y	-10.340	-5.125	-9.079	-4.515	-8.669
	CON kN	G_Y	-10.340	-3.065	-14.869	-2.455	-14.459
	CON kN	G_Y	-10.340	-3.065	-13.499	-2.455	-13.089
	CON kN	G_Y	-10.340	-3.065	-10.449	-2.455	-10.039
	CON kN	G_Y	-10.340	-3.065	-9.079	-2.455	-8.669
	CON kN	G_Y	-53.160	-5.125	-1.469	-4.515	-1.059
	CON kN	G_Y	-53.160	-3.065	-1.469	-2.455	-1.059
	CON kN	G_Y	-53.240	-5.125	-6.949	-4.515	-6.539
	CON kN	G_Y	-53.240	-5.125	-5.429	-4.515	-5.019
	CON kN	G_Y	-53.240	-3.065	-6.949	-2.455	-6.539
	CON kN	G_Y	-53.240	-3.065	-5.429	-2.455	-5.019
	CON kN	G_Y	-53.340	-5.125	-14.869	-4.515	-14.459
	CON kN	G_Y	-53.340	-5.125	-13.499	-4.515	-13.089
	CON kN	G_Y	-53.340	-5.125	-10.449	-4.515	-10.039
	CON kN	G_Y	-53.340	-5.125	-9.079	-4.515	-8.669
	CON kN	G_Y	-53.340	-3.065	-14.869	-2.455	-14.459
	CON kN	G_Y	-53.340	-3.065	-13.499	-2.455	-13.089
	CON kN	G_Y	-53.340	-3.065	-10.449	-2.455	-10.039
	CON kN	G_Y	-53.340	-3.065	-9.079	-2.455	-8.669
	CON kN	G_Y	-20.160	-5.125	-1.469	-4.515	-1.059
	CON kN	G_Y	-20.160	-3.065	-1.469	-2.455	-1.059
	CON kN	G_Y	-20.240	-5.125	-6.949	-4.515	-6.539
	CON kN	G_Y	-20.240	-5.125	-5.429	-4.515	-5.019
	CON kN	G_Y	-20.240	-3.065	-6.949	-2.455	-6.539
	CON kN	G_Y	-20.240	-3.065	-5.429	-2.455	-5.019
	CON kN	G_Y	-20.340	-5.125	-14.869	-4.515	-14.459
	CON kN	G_Y	-20.340	-5.125	-13.499	-4.515	-13.089
	CON kN	G_Y	-20.340	-5.125	-10.449	-4.515	-10.039
	CON kN	G_Y	-20.340	-5.125	-9.079	-4.515	-8.669

Source: Staad Pro v8i Design Sheet

Table 4.6: BS5400: SLS BS5400_Gen_Load N39: Disp Y -ve: Plate Loads

Plate	Type	Direction	F_a	X1 (m)	Y1 (m)	X2 (m)	Y2 (m)
26	PRE N/mm^2	G_Y	-10.011	-2.250	-15.000	1.250	15.000
	PRE N/mm^2	G_Y	-10.011	1.250	-15.000	4.750	15.000
	CON kN	G_Y	-12.930	-2.250	-15.000	-	-
	CON kN	G_Y	-12.930	-1.861	-15.000	-	-
	CON kN	G_Y	-12.930	-1.472	-15.000	-	-
	CON kN	G_Y	-12.930	-1.083	-15.000	-	-
	CON kN	G_Y	-12.930	-0.694	-15.000	-	-
	CON kN	G_Y	-12.930	-0.306	-15.000	-	-
	CON kN	G_Y	-12.930	0.083	-15.000	-	-
	CON kN	G_Y	-12.930	0.472	-15.000	-	-
	CON kN	G_Y	-12.930	0.861	-15.000	-	-
	CON kN	G_Y	-12.930	1.250	-15.000	-	-
	CON kN	G_Y	-12.930	1.250	-15.000	-	-
	CON kN	G_Y	-12.930	1.639	-15.000	-	-
	CON kN	G_Y	-12.930	2.028	-15.000	-	-
	CON kN	G_Y	-12.930	2.417	-15.000	-	-
	CON kN	G_Y	-12.930	2.806	-15.000	-	-
	CON kN	G_Y	-12.930	3.194	-15.000	-	-
	CON kN	G_Y	-12.930	3.583	-15.000	-	-
	CON kN	G_Y	-12.930	3.972	-15.000	-	-
	CON kN	G_Y	-12.930	4.361	-15.000	-	-
	CON kN	G_Y	-12.930	4.750	-15.000	-	-
	CON kN	G_Y	-82.500	-5.500	-14.040	-	-
	CON kN	G_Y	-82.500	-5.500	-12.240	-	-
	CON kN	G_Y	-82.500	-5.500	-6.240	-	-
	CON kN	G_Y	-82.500	-5.500	-4.440	-	-
	CON kN	G_Y	-82.500	-4.500	-14.040	-	-
	CON kN	G_Y	-82.500	-4.500	-12.240	-	-
	CON kN	G_Y	-82.500	-4.500	-6.240	-	-
	CON kN	G_Y	-82.500	-4.500	-4.440	-	-
	CON kN	G_Y	-82.500	-3.500	-14.040	-	-
	CON kN	G_Y	-82.500	-3.500	-12.240	-	-
	CON kN	G_Y	-82.500	-3.500	-6.240	-	-
	CON kN	G_Y	-82.500	-3.500	-4.440	-	-
	CON kN	G_Y	-82.500	-2.500	-14.040	-	-
	CON kN	G_Y	-82.500	-2.500	-12.240	-	-
	CON kN	G_Y	-82.500	-2.500	-6.240	-	-
	CON kN	G_Y	-82.500	-2.500	-4.440	-	-

Source: Staad Pro v8i Design Sheet

Table 4.7: BS5400: SLS BS5400_Gen_Load N41: Disp Y -ve: Plate Loads

Plate	Type	Direction	F_a	X1 (m)	Y1 (m)	X2 (m)	Y2 (m)
26	PRE N/mm^2	G_Y	-12.160	-5.125	-1.469	-4.515	-1.059
	PRE N/mm^2	G_Y	-12.160	-3.065	-1.469	-2.455	-1.059
	CON kN	G_Y	-15.240	-5.125	-6.949	-4.515	-6.539
	CON kN	G_Y	-15.240	-5.125	-5.429	-4.515	-5.019
	CON kN	G_Y	-15.240	-3.065	-6.949	-2.455	-6.539
	CON kN	G_Y	-15.240	-3.065	-5.429	-2.455	-5.019
	CON kN	G_Y	-15.340	-5.125	-14.869	-4.515	-14.459
	CON kN	G_Y	-15.340	-5.125	-13.499	-4.515	-13.089
	CON kN	G_Y	-87.340	-5.125	-10.449	-4.515	-10.039
	CON kN	G_Y	-87.340	-5.125	-9.079	-4.515	-8.669
	CON kN	G_Y	-87.340	-3.065	-14.869	-2.455	-14.459
	CON kN	G_Y	-87.340	-3.065	-13.499	-2.455	-13.089
	CON kN	G_Y	-87.340	-3.065	-10.449	-2.455	-10.039
	CON kN	G_Y	-87.340	-3.065	-9.079	-2.455	-8.669
	CON kN	G_Y	-87.447	-2.390	-5.303	-2.010	-5.103
	CON kN	G_Y	-87.447	-2.390	-2.303	-2.010	-2.103
	CON kN	G_Y	-87.447	-2.390	0.697	-2.010	0.897
	CON kN	G_Y	-87.447	-2.390	3.697	-2.010	3.897
	CON kN	G_Y	-87.447	-0.590	-5.303	-0.210	-5.103
	CON kN	G_Y	-87.447	-0.590	-2.303	-0.210	-2.103
	CON kN	G_Y	-87.447	-0.590	0.697	-0.210	0.897
	CON kN	G_Y	-87.447	-0.590	3.697	-0.210	3.897
	CON kN	G_Y	-21.450	-2.300	-14.978	-2.100	-14.828
	CON kN	G_Y	-21.450	-2.300	-13.878	-2.100	-13.728
	CON kN	G_Y	-21.450	-0.500	-14.978	-0.300	-14.828
	CON kN	G_Y	-21.450	-0.500	-13.878	-0.300	-13.728
	CON kN	G_Y	-21.456	-2.450	-10.728	-1.950	-10.478
	CON kN	G_Y	-21.456	-2.450	-9.628	-1.950	-9.378
	CON kN	G_Y	-21.456	-0.650	-10.728	-0.150	-10.478
	CON kN	G_Y	-21.456	-0.650	-9.628	-0.150	-9.378
	CON kN	G_Y	-21.160	-5.125	-1.469	-4.515	-1.059
	CON kN	G_Y	-21.160	-3.065	-1.469	-2.455	-1.059
	CON kN	G_Y	-21.240	-5.125	-6.949	-4.515	-6.539
	CON kN	G_Y	-21.240	-5.125	-5.429	-4.515	-5.019
	CON kN	G_Y	-21.240	-3.065	-6.949	-2.455	-6.539
	CON kN	G_Y	-21.240	-3.065	-5.429	-2.455	-5.019
	CON kN	G_Y	-21.340	-5.125	-14.869	-4.515	-14.459
	CON kN	G_Y	-21.340	-5.125	-13.499	-4.515	-13.089

Source: Staad Pro v8i Design Sheet

Table 4.8: BS5400: SLS BS5400_Gen_Load N42: Disp Y -ve: Plate Loads

Plate	Type	Direction	F_a	X1 (m)	Y1 (m)	X2 (m)	Y2 (m)
26	PRE N/mm^2	G_Y	-10.160	-5.125	-1.469	-4.515	-1.059
	PRE N/mm^2	G_Y	-10.160	-3.065	-1.469	-2.455	-1.059
	CON kN	G_Y	-83.240	-5.125	-6.949	-4.515	-6.539
	CON kN	G_Y	-83.240	-5.125	-5.429	-4.515	-5.019
	CON kN	G_Y	-83.240	-3.065	-6.949	-2.455	-6.539
	CON kN	G_Y	-83.240	-3.065	-5.429	-2.455	-5.019
	CON kN	G_Y	-83.340	-5.125	-14.869	-4.515	-14.459
	CON kN	G_Y	-83.340	-5.125	-13.499	-4.515	-13.089
	CON kN	G_Y	-83.340	-5.125	-10.449	-4.515	-10.039
	CON kN	G_Y	-83.340	-5.125	-9.079	-4.515	-8.669
	CON kN	G_Y	-83.340	-3.065	-14.869	-2.455	-14.459
	CON kN	G_Y	-83.340	-3.065	-13.499	-2.455	-13.089
	CON kN	G_Y	-83.340	-3.065	-10.449	-2.455	-10.039
	CON kN	G_Y	-83.340	-3.065	-9.079	-2.455	-8.669
	CON kN	G_Y	-16.447	-2.390	-5.303	-2.010	-5.103
	CON kN	G_Y	-16.447	-2.390	-2.303	-2.010	-2.103
	CON kN	G_Y	-16.447	-2.390	0.697	-2.010	0.897
	CON kN	G_Y	-16.447	-2.390	3.697	-2.010	3.897
	CON kN	G_Y	-16.447	-0.590	-5.303	-0.210	-5.103
	CON kN	G_Y	-16.447	-0.590	-2.303	-0.210	-2.103
	CON kN	G_Y	-16.447	-0.590	0.697	-0.210	0.897
	CON kN	G_Y	-16.447	-0.590	3.697	-0.210	3.897
	CON kN	G_Y	-16.450	-2.300	-14.978	-2.100	-14.828
	CON kN	G_Y	-16.450	-2.300	-13.878	-2.100	-13.728
	CON kN	G_Y	-16.450	-0.500	-14.978	-0.300	-14.828
	CON kN	G_Y	-16.450	-0.500	-13.878	-0.300	-13.728
	CON kN	G_Y	-16.456	-2.450	-10.728	-1.950	-10.478
	CON kN	G_Y	-16.456	-2.450	-9.628	-1.950	-9.378
	CON kN	G_Y	-16.456	-0.650	-10.728	-0.150	-10.478
	CON kN	G_Y	-16.456	-0.650	-9.628	-0.150	-9.378
	CON kN	G_Y	-16.160	-5.125	-1.469	-4.515	-1.059
	CON kN	G_Y	-16.160	-3.065	-1.469	-2.455	-1.059
	CON kN	G_Y	-31.240	-5.125	-6.949	-4.515	-6.539
	CON kN	G_Y	-31.240	-5.125	-5.429	-4.515	-5.019
	CON kN	G_Y	-31.240	-3.065	-6.949	-2.455	-6.539
	CON kN	G_Y	-31.240	-3.065	-5.429	-2.455	-5.019
	CON kN	G_Y	-31.340	-5.125	-14.869	-4.515	-14.459
	CON kN	G_Y	-31.340	-5.125	-13.499	-4.515	-13.089

Source: Staad Pro v8i Design Sheet

Table 4.9: BS5950: Load Factor of Safety

Comb.	Combination L/C Name	Primary L/C Name	Factor
9	Generated British BS5950 1	Dead Load Case 1	1.40
		HB Loading	1.60
10	Generated British BS5950 1	Dead Load Case 1	1.35
		HB Loading	1.55
11	Generated British BS5950 1	Dead Load Case 1	1.50
12	Generated British BS5950 1	Dead Load Case 1	1.20

Source: Staad Pro v8i Design Sheet

Table 4.10: Node Displacements Summary

	Node	L/C	X (mm)	Y (mm)	Z (mm)	Resultant (mm)	rX (rad)	rY (rad)	rZ (rad)
Max X	19	9: Generate	1.3+15	-7.97+15	0.0	8.07+15	0.000	0.000	-124E+9
Min X	23	9: Generate	-1.21+15	-8.83+15	0.0	8.91+15	0.000	0.000	-15.5E+9
Max Y	39	9: Generate	0.000	19.2+18	0.0	19.2+18	530 +12	0.000	-203+12
Min Y	39	2:BS5400: SLS	0.000	-5.66+18	0.0	5.66+18	-154+12	0.000	65.5+12
Max Z	1	1: Dead Load	0.002	-0.010	0.0	0.010	0.000	0.000	0.000
Min Z	1	1: Dead Load	0.002	-0.010	0.0	0.010	0.000	0.000	0.000
Max r_X	39	9: Generate	0.000	19.2+18	0.0	19.2+18	530 +12	0.000	-203+12
Min r_X	39	2:BS5400: SLS	0.000	-5.66+18	0.0	5.66+18	-154+12	0.000	65.5+12
Max r_Y	1	1: Dead Load	0.002	-0.010	0.0	0.010	0.000	0.000	0.000
Min r_Y	1	1: Dead Load	0.002	-0.010	0.0	0.010	0.000	0.000	0.000
Max r_Z	39	2:BS5400: SLS	0.000	-5.66+18	0.0	5.66+18	-154+12	0.000	65.5+12
Min r_Z	39	9: Generate	0.000	19.2+18	0.0	19.2+18	530 +12	0.000	-203+12
Max R_{st}	39	9: Generate	0.000	19.2+18	0.0	19.2+18	530 +12	0.000	-203+12

Source: Staad Pro v8i Design Sheet

Table 4.11: Node Displacements Summary

	Beam	L/C	d (m)	X (mm)	Y (mm)	Z (mm)	Resultant (mm)
Max X	10	9: Generate	0.000	1.37+15	-7.97+15	0.000	8.08+15
Min X	12	9: Generate	0.000	-1.2+15	-8.83+15	0.000	8.91+15
Max Y	1	1: Dead Load	2.000	0.000	0.000	0.000	0.000
Min Y	10	9: Generate	14.000	1.37+15	-9.7+15	0.000	9.8+15
Max Z	24	1: Dead Load	21.000	0.000	-8.184	0.001	8.184
Min Z	23	1: Dead Load	21.000	0.000	-8.184	-0.001	8.184
Max R_{st}	10	9: Generate	14.000	1.37+15	-9.7+15	0.000	9.8+15

Source: Staad Pro v8i Design Sheet

Table 4.12: Node Displacements Summary

	Node	L/C	X (mm)	Y (mm)	Z (mm)	Resultant (mm)	r_X (rad)	r_Y (rad)	r_Z (rad)
Max X	19	1: Dead Load	0.426	-106E+6	0.000	106E+6	0.000	0.0	3.94E+3
Min X	25	1: Dead Load	-0.850	-106E+6	0.000	106E+6	0.000	0.0	3.94E+3
Max Y	33	1: Dead Load	0.000	0.000	0.000	0.000	0.000	0.0	0.000
Min Y	39	1: Dead Load	0.000	-97.7E+9	0.000	97.7E+9	-2.53E+6	0.0	969E+3
Max Z	1	1: Dead Load	0.001	-0.005	0.000	0.005	0.000	0.0	0.000
Min Z	1	1: Dead Load	0.001	-0.005	0.000	0.005	0.000	0.0	0.000
Max r_X	1	1: Dead Load	0.001	-0.005	0.000	0.005	0.000	0.0	0.000
Min r_X	40	1: Dead Load	0.000	-84.1E+9	0.000	84.1E+9	-2.53E+6	0.0	969E+3
Max r_Y	1	1: Dead Load	0.001	-0.005	0.000	0.005	0.000	0.0	0.000
Min r_Y	1	1: Dead Load	0.001	-0.005	0.000	0.005	0.000	0.0	0.000
Max r_Z	41	1: Dead Load	0.000	-21.8E+9	0.000	21.8E+9	-2.53E+6	0.0	969E+3
Min r_Z	5	1: Dead Load	-0.847	-51.3E+6	0.000	51.3E+6	0.000	0.0	-3.94E+3
Max R_{st}	39	1: Dead Load	0.000	-97.7E+9	0.000	97.7E+9	-2.53E+6	0.0	969E+3

Source: Staad Pro v8i Design Sheet

Table 4.13: Plate Centre Stress Summary

	Plate	L/C	Q_x (N/mm^2)	Q_y (N/mm^2)	M_x (kN^-m/m)	M_y (kN^-m/m)	M_{xy} (kN^-m/m)
Max Q_x	26	9: Generate	2.463	0.328	-788.997	-9.34E+3	-2.5E+3
Min Q_x	26	BS5400: SLS	-0.766	0.301	-102.069	-3E+3	-702.934
Max Q_y	26	9: Generate	2.463	0.328	-788.997	-9.34E+3	-2.5E+3
Min Q_y	26	2:BS5400: SLS	-0.055	-0.055	338.050	-19.652	861.253
Max S_x	26	1: Dead Load	1.642	0.219	-525.998	-6.23E+3	-1.67E+3
Min S_x	26	1: Dead Load	1.642	0.219	-525.998	-6.23E+3	-1.67E+3
Max S_y	26	1: Dead Load	1.642	0.219	-525.998	-6.23E+3	-1.67E+3
Min S_y	26	1: Dead Load	1.642	0.219	-525.998	-6.23E+3	-1.67E+3
Max S_{xy}	26	1: Dead Load	1.642	0.219	-525.998	-6.23E+3	-1.67E+3
Min S_{xy}	26	1: Dead Load	1.642	0.219	-525.998	-6.23E+3	-1.67E+3
Max M_x	26	2:BS5400: SLS	-0.055	-0.055	338.050	-19.652	861.253
Min M_x	26	9: Generate	2.463	0.328	-788.997	-9.34E+3	-2.5E+3
Max M_y	26	3:BS5400: SLS	0.000	0.000	0.000	0.000	0.000
Min M_y	26	9: Generate	2.463	0.328	-788.997	-9.34E+3	-2.5E+3
Max M_{xy}	26	2:BS5400: SLS	-0.055	-0.055	338.050	-19.652	861.253
Min M_{xy}	26	9: Generate	2.463	0.328	-788.997	-9.34E+3	-2.5E+3

Source: Staad Pro v8i Design Sheet

Table 4.14: Plate Center Principal Stress Summary

			Principal		Von Mis		Tresca	
	Plate	**L/C**	**Top** (N/mm^2)	**Bottom** (N/mm^2)	**Top** (N/mm^2)	**Bottom** (N/mm^2)	**Top** (N/mm^2)	**Bottom** (N/mm^2)
Max (t)	26	1: Dead Load	-79.576	551.880	516.709	516.709	551.880	551.880
Max (b)	26	1: Dead Load	-79.576	551.880	516.709	516.709	551.880	551.880
Max V_M (t)	26	1: Dead Load	-79.576	551.880	516.709	516.709	551.880	551.880
Max V_M (b)	26	1: Dead Load	-79.576	551.880	516.709	516.709	551.880	551.880
Tresca (t)	26	1: Dead Load	-79.576	551.880	516.709	516.709	551.880	551.880
Tresca (b)	26	1: Dead Load	-79.576	551.880	516.709	516.709	551.880	551.880

Source: Staad Pro v8i Design Sheet

Table 4.15: Reaction Summary

			Horizontal	Vertical	Horizontal	Moment		
	Node	**L/C**	**F_X** (KN)	**F_Y** (KN)	**F_Z** (KN)	**M_X** (KN.m)	**M_Y** (KN.m)	**M_Z** (KN.m)
Max F_X	33	1: Dead Load	0.000	62.721	0.000	-184.252	0.000	0.479
Min F_X	33	1: Dead Load	0.000	62.721	0.000	-184.252	0.000	0.479
Max F_Y	37	9: Generate	0.000	98.393	0.000	-276.377	0.000	0.000
Min F_Y	33	2:BS5400: SLS	0.000	0.000	0.000	0.000	0.000	0.000
Max F_Z	33	1: Dead Load	0.000	62.721	0.000	-184.252	0.000	0.479
Min F_Z	33	1: Dead Load	0.000	62.721	0.000	-184.252	0.000	0.479
Max M_X	35	9: Generate	0.000	94.082	0.000	276.377	0.000	0.719
Min M_X	33	9: Generate	0.000	94.082	0.000	-276.377	0.000	0.719
Max M_Y	33	1: Dead Load	0.000	62.721	0.000	-184.252	0.000	0.479
Min M_Y	33	1: Dead Load	0.000	62.721	0.000	-184.252	0.000	0.479
Max M_Z	33	9: Generate	0.000	94.082	0.000	-276.377	0.000	0.719
Min M_Z	34	9: Generate	0.000	94.082	0.000	-276.377	0.000	-0.719

Source: Staad Pro v8i Design Sheet

Table 4.16: Beam End Displacement Summary

	Beam	**Node**	**L/C**	**X** (mm)	**Y** (mm)	**Z** (mm)	**Resultant** (mm)
Max X	3	5	1: Dead Load	2.36E+6	-51.3E+6	0.000	51.4E+6
Min X	13	25	1: Dead Load	-2.36E+6	-106E+6	0.000	107E+6
Max Y	1	33	1: Dead Load	0.000	0.000	0.000	0.000
Min Y	3	6	1: Dead Load	2.36E+6	-106E+6	0.000	107E+6
Max Z	1	1	1: Dead Load	0.000	-0.005	0.000	0.005
Min Z	1	1	1: Dead Load	0.000	-0.005	0.000	0.005
Max R_{st}	3	6	1: Dead Load	2.36E+6	-106E+6	0.000	107E+6

Source: Staad Pro v8i Design Sheet

Table 4.17: Reaction Envelope

		Horizontal	Vertical	Horizontal	Moment		
Node	**Env**	**Fx** (kN)	**Fy** (kN)	**Fz** (kN)	**Mx** (kNm)	**My** (kNm)	**Mz** (kNm)
33	+ve	0.000	41.878	0.000	0.000	0.000	0.093
33	+ve	-	Load: 1	-	-	-	Load: 1
33	-ve	0.000	0.000	0.000	-184.252	0.000	0.000
34	+ve	0.000	41.878	0.000	0.000	0.000	0.000
34	+ve	-	Load: 1	-	-	-	-
34	-ve	0.000	0.000	0.000	-184.252	0.000	-0.093
34	-ve	-	-	-	Load: 1	-	Load: 1
35	+ve	0.000	41.878	0.000	184.252	0.000	0.093
35	+ve	-	Load: 1	-	Load: 1	-	Load: 1
35	-ve	0.000	0.000	0.000	0.000	0.000	0.000
35	-ve	-	-	-	-	-	-
36	+ve	0.000	41.878	0.000	184.252	0.000	0.000
36	+ve	-	Load: 1	-	Load: 1	-	-
36	-ve	0.000	0.000	0.000	0.000	0.000	-0.093
36	-ve	-	-	-	-	-	Load: 1
37	+ve	0.000	42.436	0.000	0.000	0.000	0.000
37	+ve	-	Load: 1	-	-	-	Load: 1
37	-ve	0.000	0.000	0.000	-184.252	0.000	0.000
37	-ve	-	-	-	Load: 1	-	-
38	+ve	0.000	42.436	0.000	184.252	0.000	0.000
38	+ve	-	Load: 1	-	Load: 1	-	Load: 1
38	-ve	0.000	0.000	0.000	0.000	0.000	0.000
38	-ve	-	-	-	-	-	-

Source: Staad Pro v8i Design Sheet

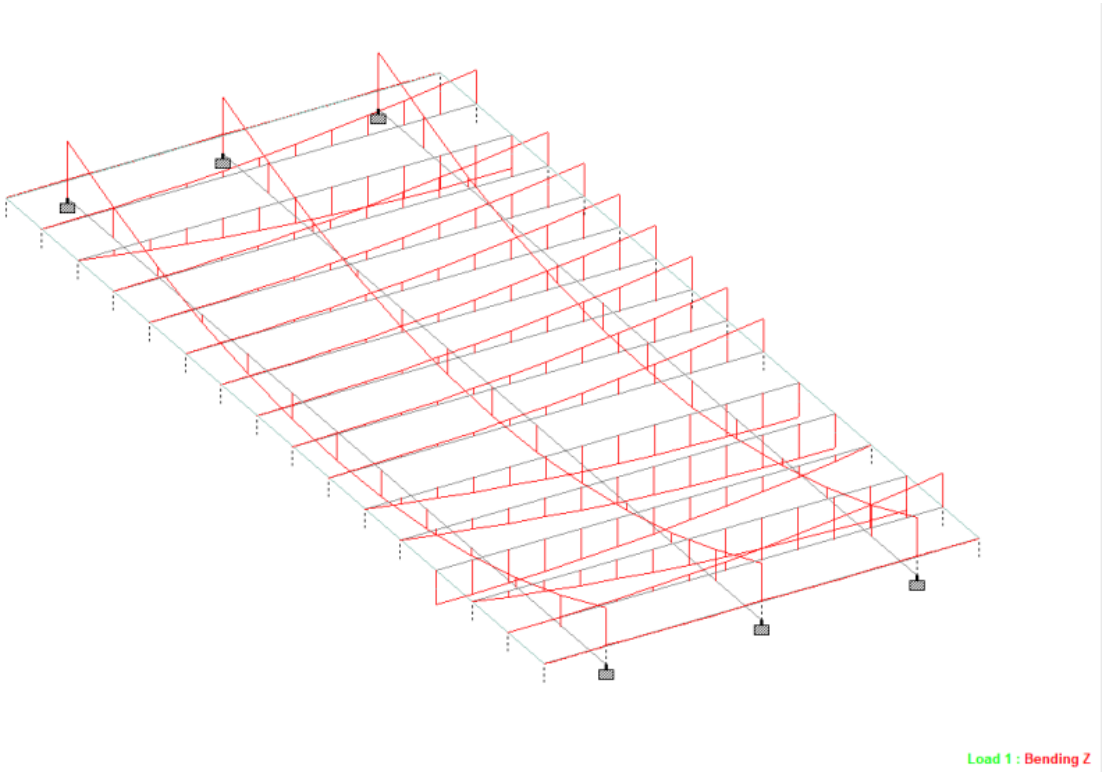

Fig 4.1: Bending Moment transverse and longitudinal stress diagram at deck plate centre

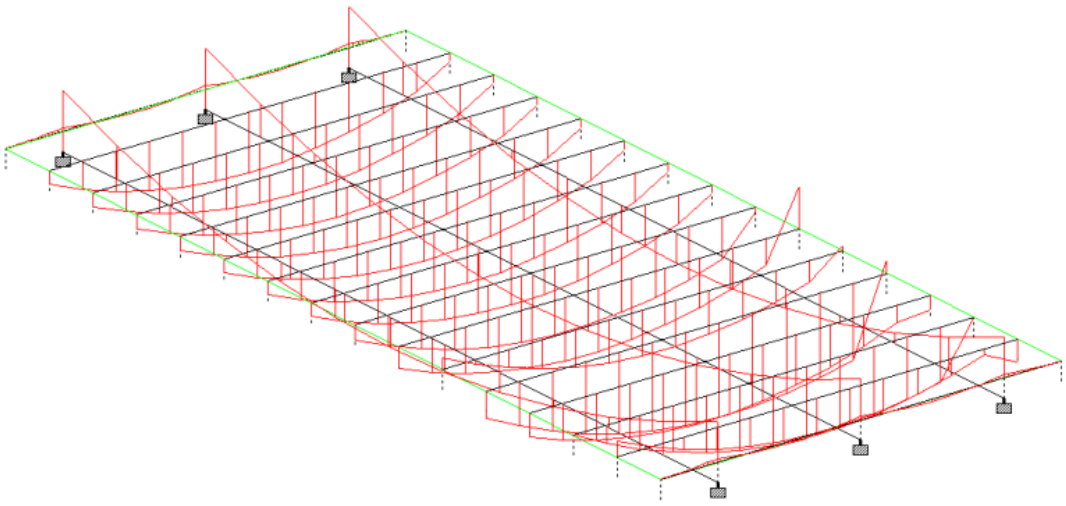

Fig 4.2: Bending Moment and Shear Force for transverse and longitudinal beam at deck plate centre

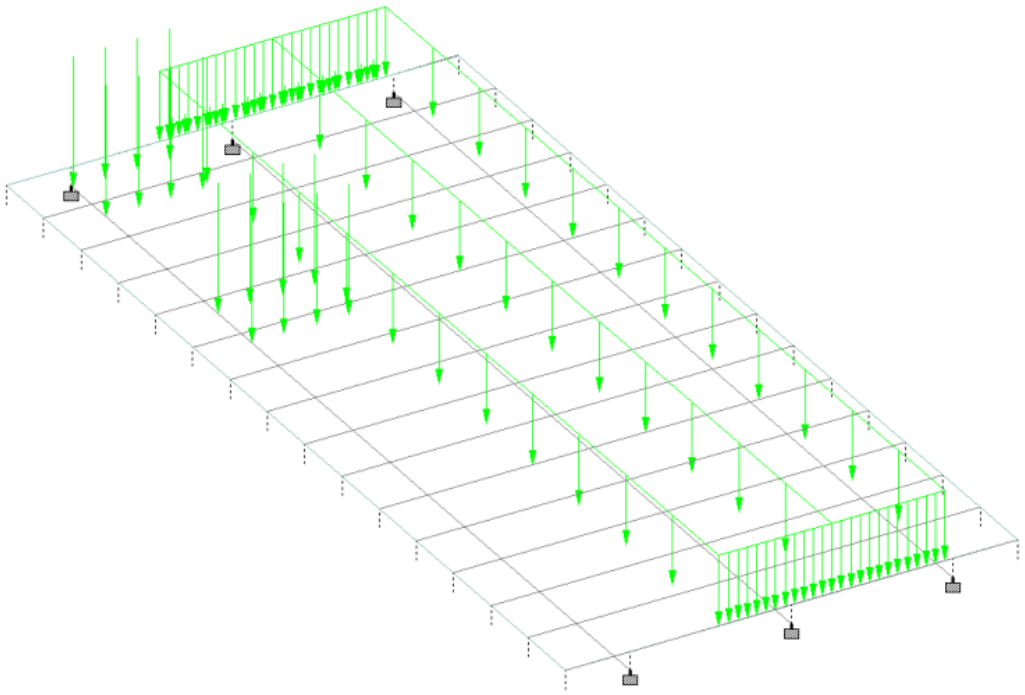

Fig 4.3: Bridge Deck showing HA and HB loading range (MPa)

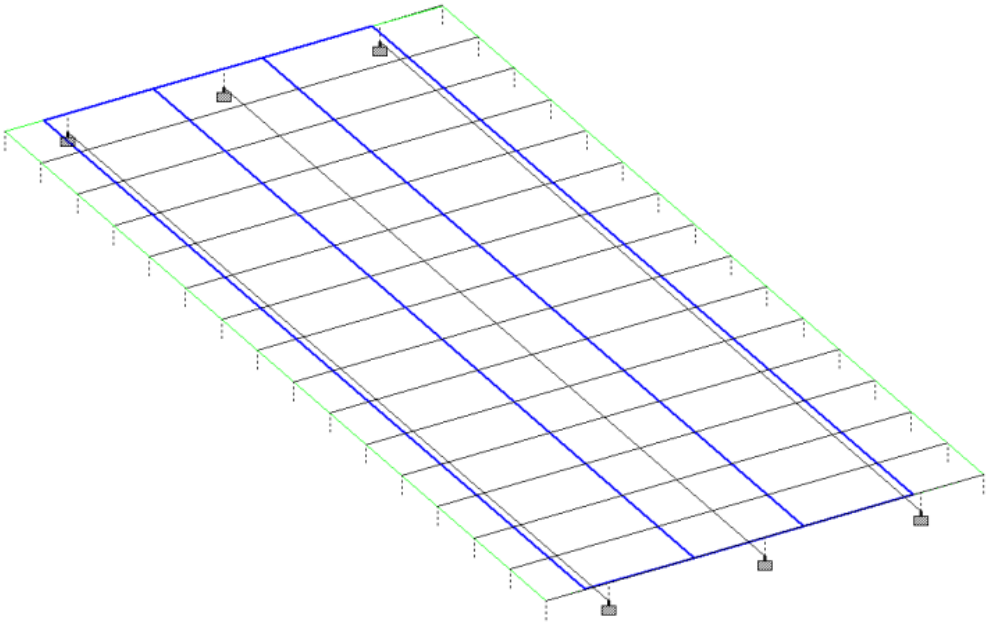

Fig 4.4: Bridge Deck showing HA and HB loading roadway

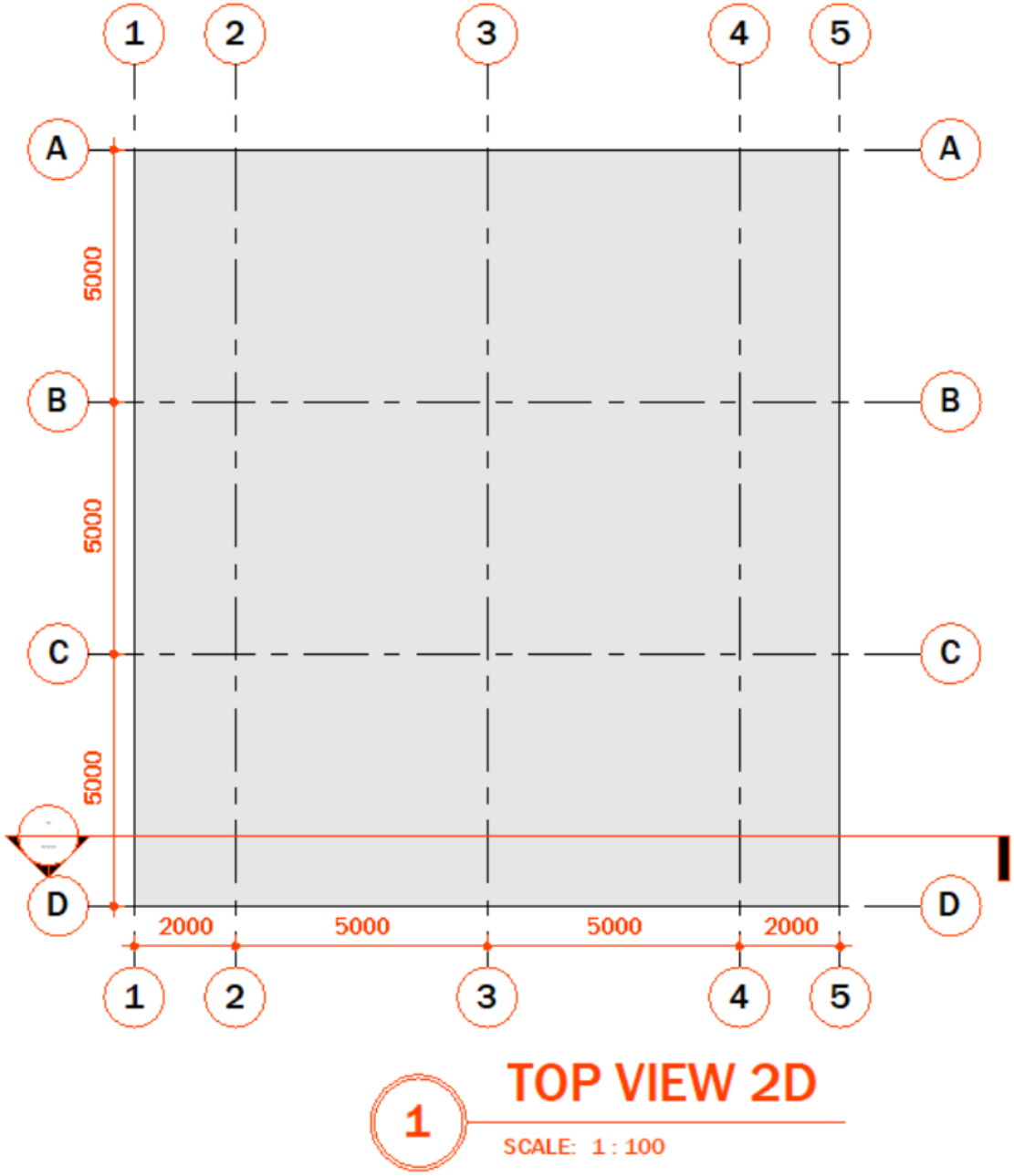

Fig 4.5: 2D View of Bridge Deck

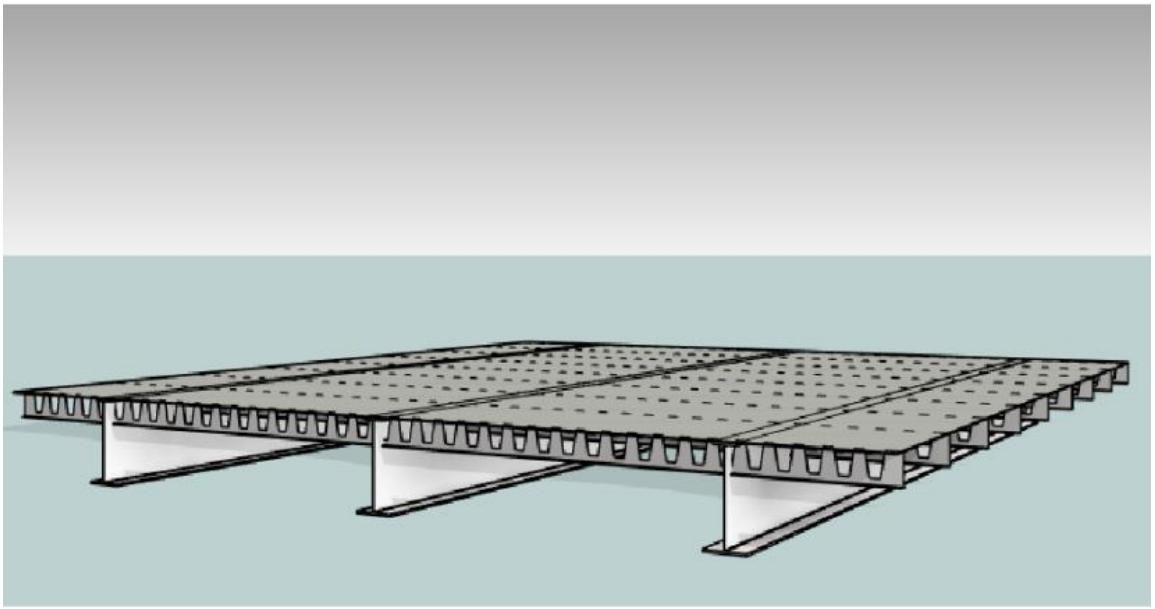

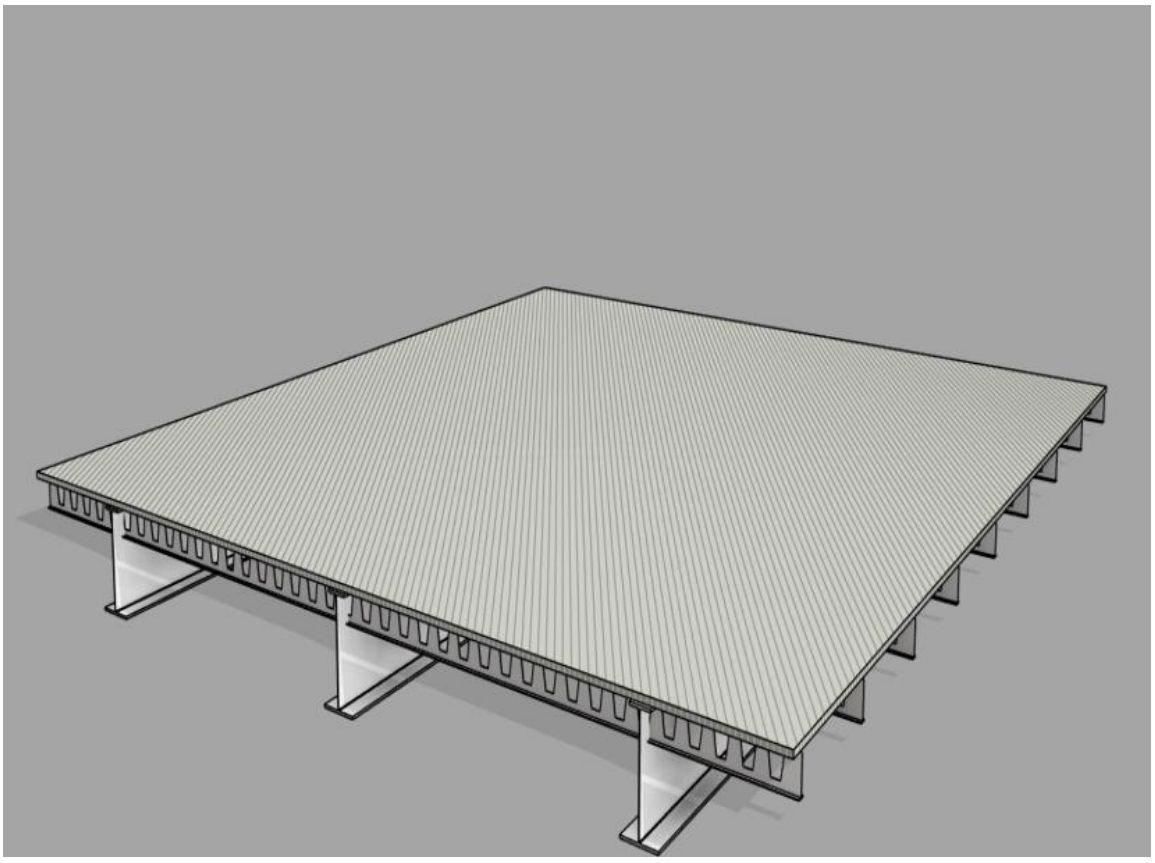

Fig 4.6: 3D View of Bridge Deck

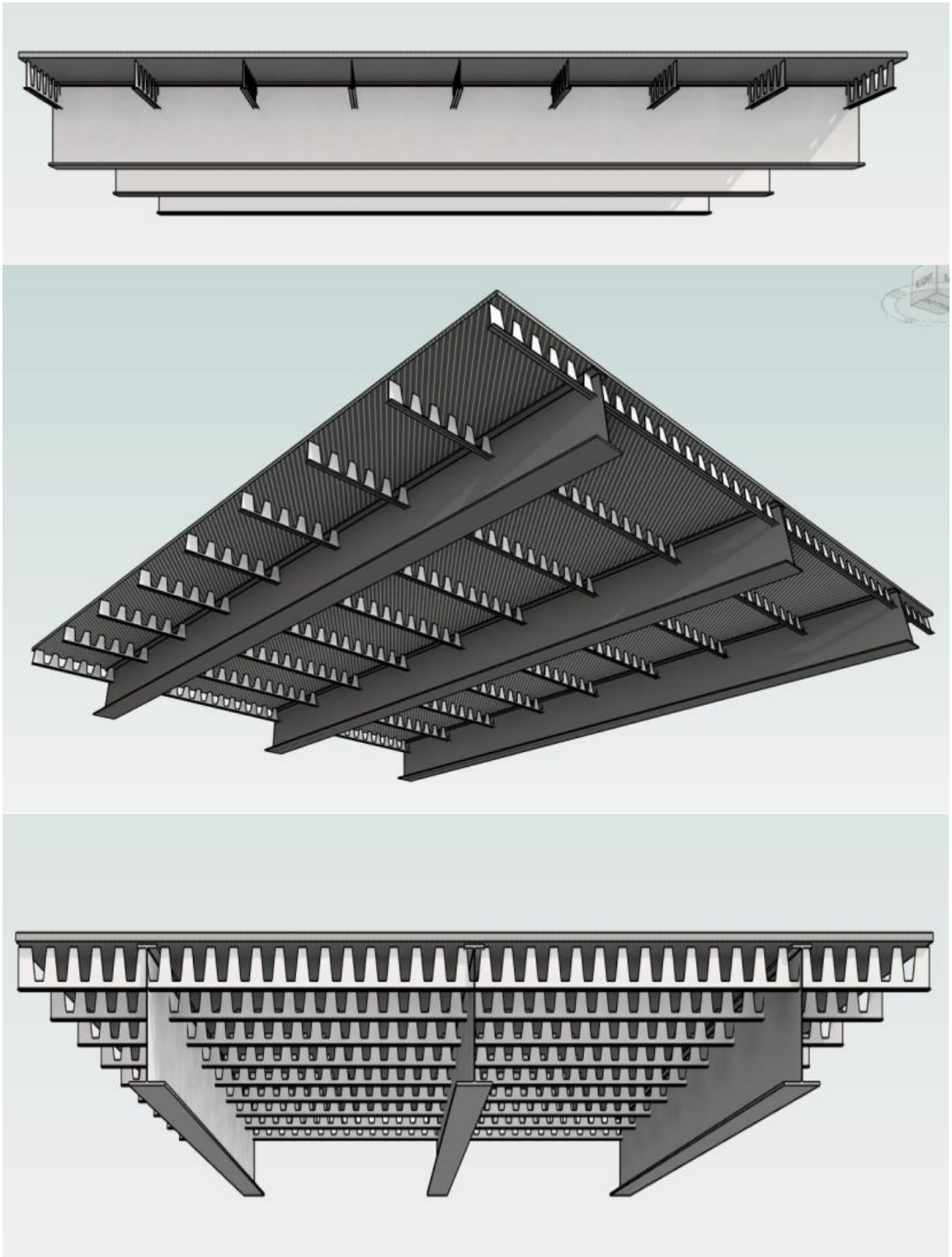

Fig 4.7: 3D View of Bridge Deck

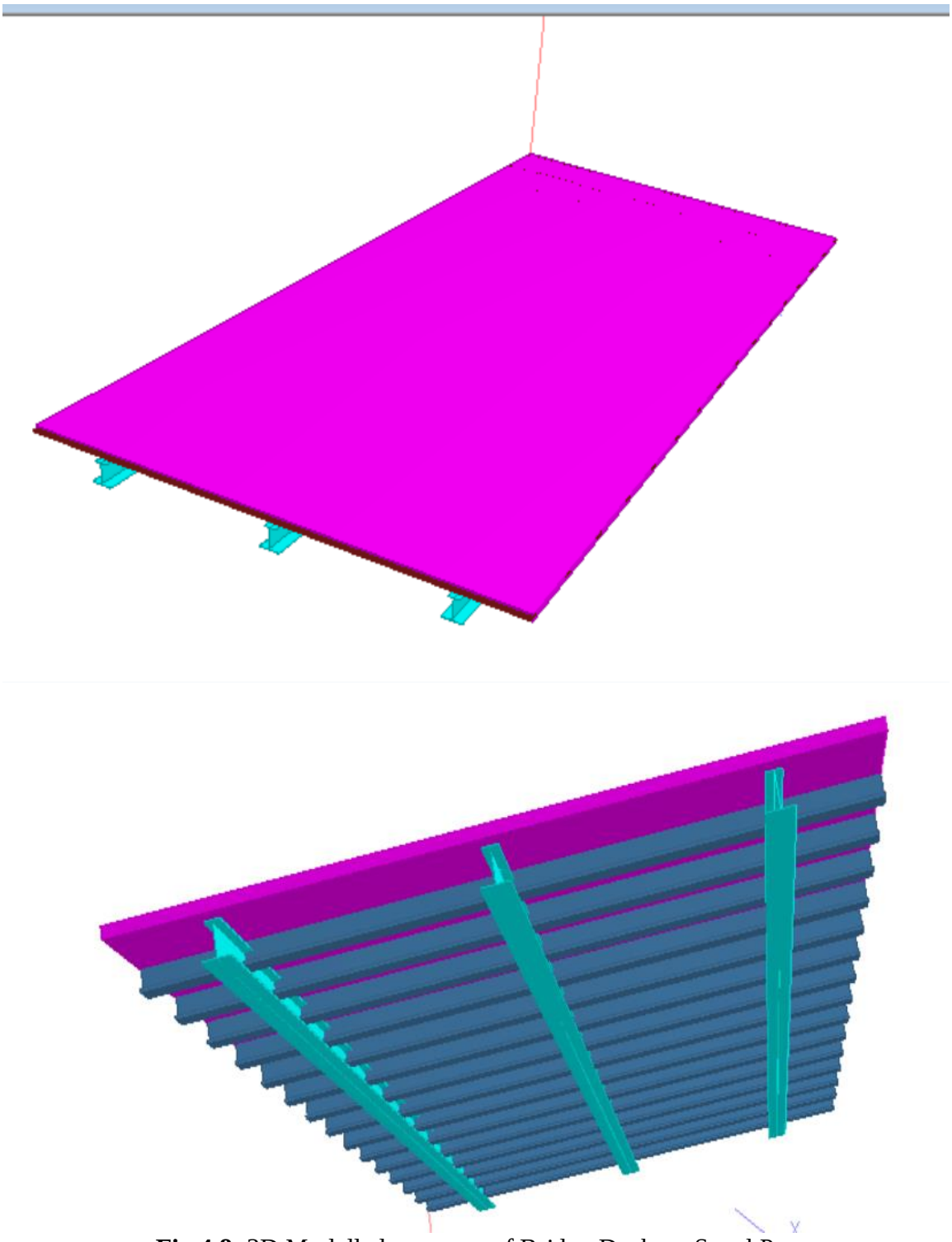

Fig 4.8: 3D Modelled structure of Bridge Deck on Staad Pro

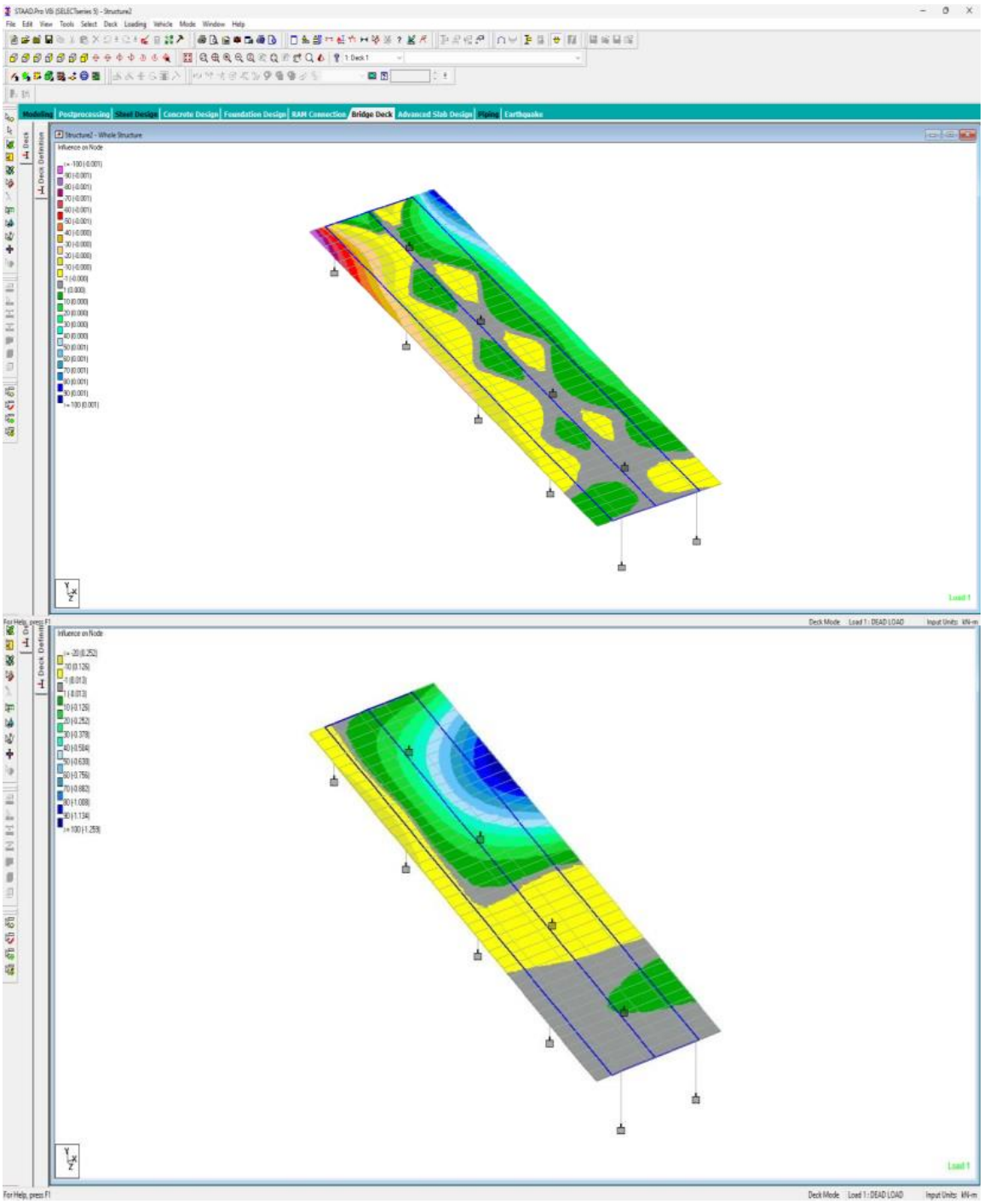

Fig 4.9: Transverse and Longitudinal stress on Bridge Due to Dead Load

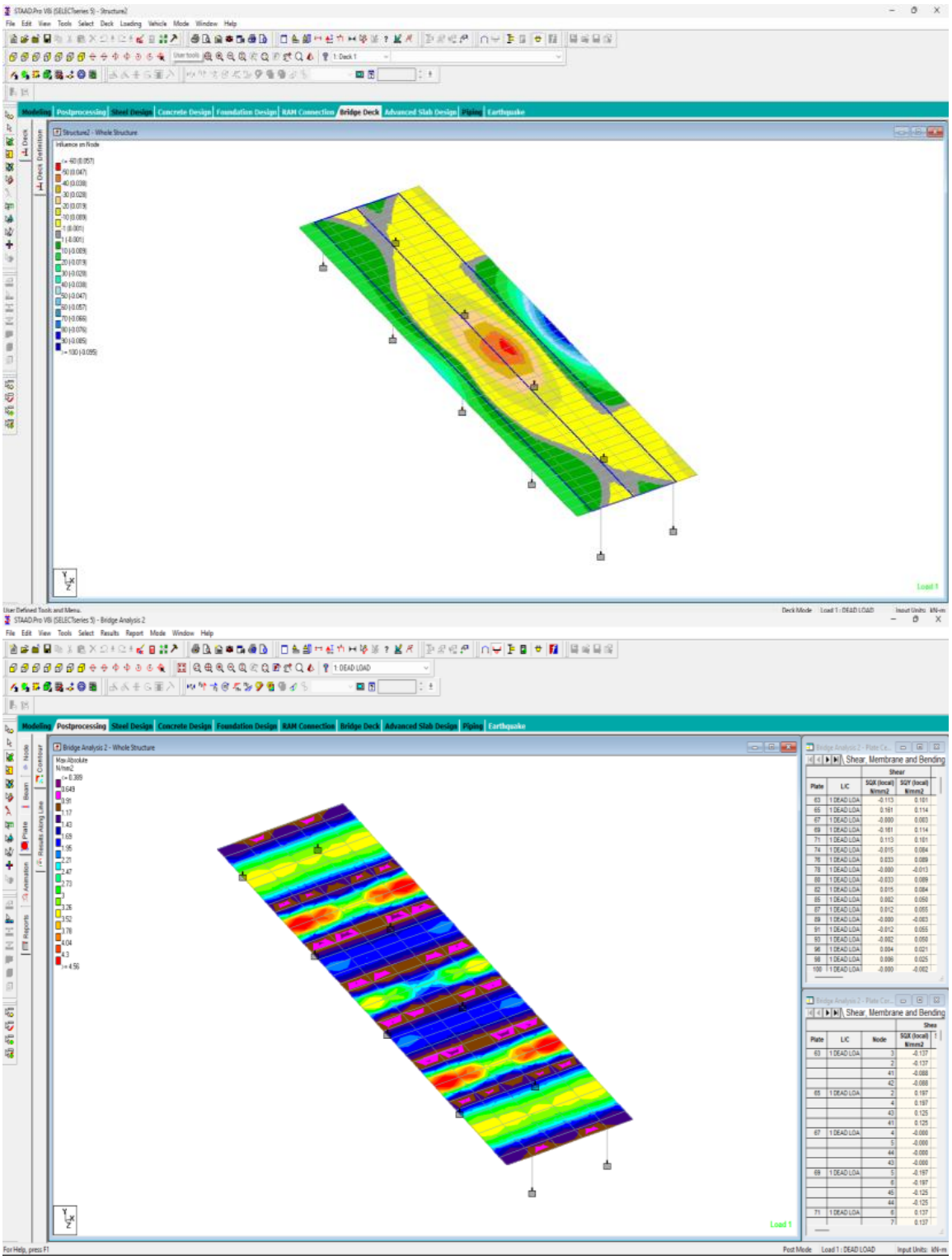

Fig 4.10: Maximum Transverse and Longitudinal stress on Bridge Due to HA and HB Loading

4.3 Results from Morrice and Little Design Curve Approach

The Morrice and Little method provided initial estimates for load capacity and stress distribution in the orthotropic bridge decks.

4.3.1 Analysis and Design of Deck Slab

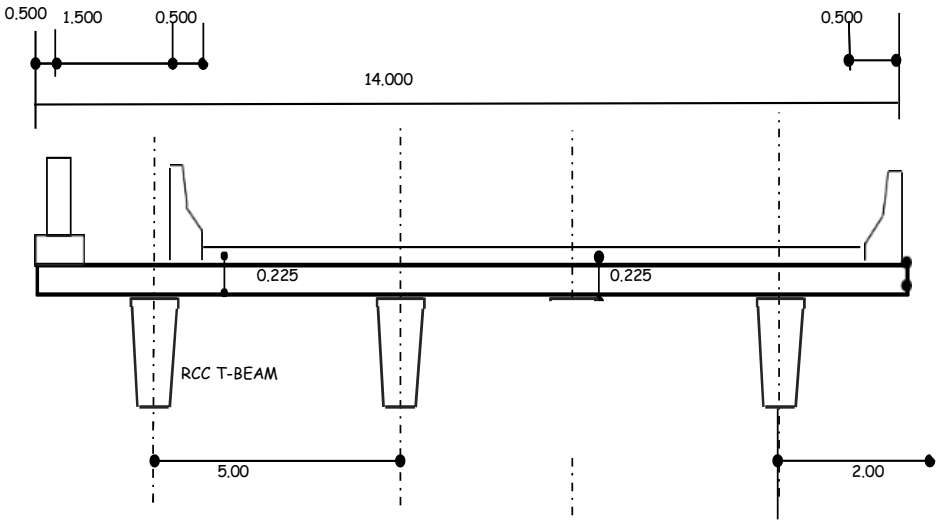

The deck slab was analysed in the transverse direction as a continuous slab system supported on longitudinal girders, with cantilever overhangs on both sides. To simplify the analysis while capturing the essential behaviour, a unit-width strip of the deck was considered along the span, a common approach in orthotropic deck design. This allowed for detailed evaluation of transverse bending and shear behaviour under various loading conditions. The structural analysis considered multiple loading types in compliance with relevant design codes: Dead Load (DL), Superimposed Dead Load (SIDL), Footpath Live Load (FPLL), and Carriageway Live Load (CWLL). These loads were applied to simulate real-world service conditions. Additionally, to capture the effect of load transfer and rotational restraint at supports, equivalent forces and moments were applied at the ends of the slab strip, representing boundary effects from adjacent structural elements.

The entire transverse analysis was conducted using STAADPro v8i, which enabled precise modelling of slab geometry, boundary conditions, and loading configurations.

Table 4.18: Bridge Geometry and Material Properties

Design Data:			
Total Width of Superstructure	=	14.000 m	
Width of Carriageway	=	7.500 m	
Effective Span	=	30.000 m	
Width of Railing	=	0.500 m	
Width of Footway	=	1.500 m	
Width of C/Barrier on Footpath side	=	0.500 m	
Width of C/Barrier on Median side	=	0.500 m	
Skew angle	=	21.000	
Thickness of Deck slab at centre	=	0.225 m	
Thickness of Deck slab at cantilever root Thickness	=	0.225 m	
of Deck slab at cant end	=	0.225 m	
Nos. of Transverse Girders	=	3	
C/C spacing of Transverse girders	=	5.000 m	
Width of girder Flange at top=		0.350 m	
Width of girder Flange at bottom	=	0.600 m	
Overhang of Deck slab at support	=	1.500 m (from c/l of T. Girder)	
Thickness of wearing coat	=	0.100 m	
Depth of haunch	=	0.075 m	
Material Properties:			
~~Grade of Concrete Used~~	=	~~C40~~	
~~Grade of steel~~		~~Fe 460~~	
Characteristic strength of concrete (f_{ck})	=	40 MPa	Table no:6.5 (BS5400)
Characteristic strength of steel (f_y)	=	460 MPa	Table no:18.1 (BS5400)
Tensile strength of concrete (f_{ctm})	=	4 MPa	Table no:6.5 BS5400)
Design yield strength of shear reinforcement f_{ywd} = 0	=	350 MPa	Page 86 BS5400
Partial material safety factor for concrete (y_m)	=	1.4 DL + 1.6 LL	Page 49: BS5400
Partial material safety factor for Steel (y_s)	=	1.15 Basic	Page 30: BS5400
Ultimate compressive strain in the concrete (ϵ_{cu3})	=	0.0035 Up to fck ≤	Table no:6.5 BS5400
modulus of elasticity of reinforcing of steel (E_s)	=	200000 MPa	Clause 6.2.2 (BS8110)
modulus of elasticity of concrete (Ecm)	=	20000 MPa	Table no:6.5 (BS8110)
modular ratio α_e (Es/Ecm)	=	6.06	page-126 BS8110
Ultimate tensile strain in the steel (ϵ_s) = [{f_{ys}/xE_s)	=		0.00417
Coefficient to consider the influence of the concrete	=	0.67 Cube	A2.10 244 BS5400
Factor (ƙ)	=	0.8 0.8 Up to fck ≤ 60Mpa,Eq.A2-33 BS5400; 0.8-((fck-60)/500) for 60<fck	

Factor (η)	=	1 1.0 Up to fck ≤ 60Mpa,Eq.A2-35 (BS5400); 1.0-((fck-60)/250) for 60<fck<	
$f_{cd} = (\alpha * f_{ck}/y_{m)}$	=	17.867	page-49 BS5400
Factor F_{av} (η f_{cd} ƛ)	=	14.293	
Factor β = (ƛ /2)	=	0.400	
Cover	=	40 mm	

4.3.2 Load Calculation

Dead Load (Self Weight)

Self-weight of the structure is automatically calculated by Staad itself

Super Imposed Dead Load

Weight Of Wearing Coat:

Thickness of wearing coat = 0.1m

Unit weight of wearing coat = 22KNm^3

Load due to wearing coat = 2.2 KN/m^2

Weight Of Crash Barrier:

weight of crash barrier median side = 7.2KN/m

weight of crash barrier = 14.40KN/m

weight of crash barrier footpath side = 7.2KN/m

weight of crash barrier footpath side = 14.40KN/m

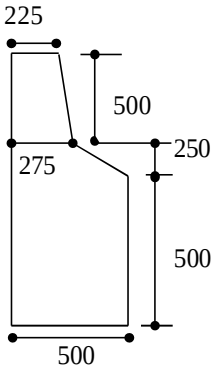

Weight Of RCC Railing:

weight of RCC kerb + steel railing = 7.2KN/m

weight of RCC kerb + steel railing = 14.58KN/m^2

Carriageway Live Load: as per BS 5400

$b_{eff} = \alpha * a * (1 - a / L) + b1$ For Continuous span

$b_{eff} = 1.2 * a + b1$ For Cantilever portion

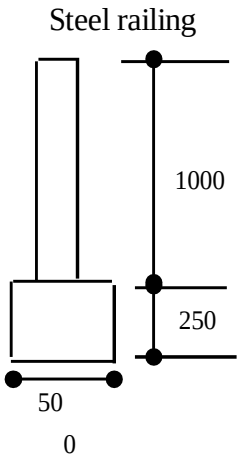

For Continuous Span:

L = 2.3 m

a = Distance of the concentrated load from C/L of nearest support

b1 = Width of the load parallel to support + 2 x thk of WC

For cantilever span

L = 1.500m

a = Distance of the concentrated load from face of the support

b1 = Width of the load parallel to support + 2 x thk of WC

Impact Factor:

For Continuous span = HA × 1.5

HB (30 units) × 1.25

For Cantilever span = HA × 1.5

HB (30 units) × 1.25

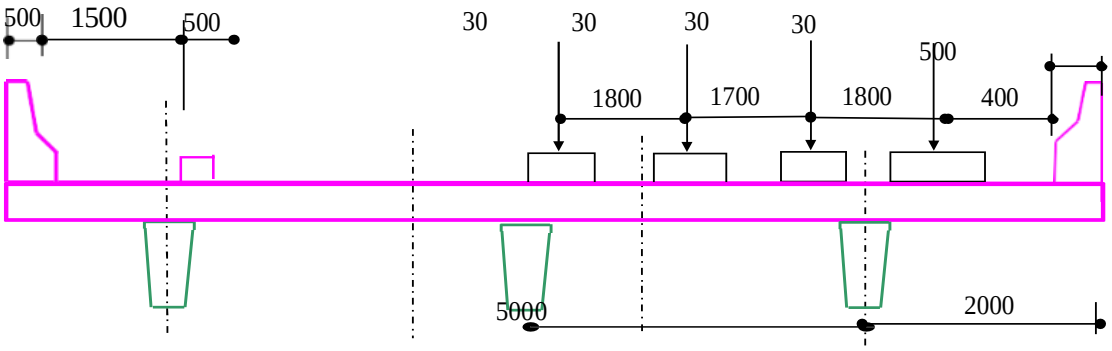

1st Load

a1 = 0.6 m b1 = 0.45 m

b_{eff} = 1.1700 < 1.2 b_{eff} (modified) = 1.170m

Load per meter width = 73.08KN

2nd Load

a1 = 1.200 m b1 = 0.45 m α = 2.60

b_{eff} = 2.32 > 1.2 b_{eff} (modified) = 1.76m

Load per meter width = 48.55KN

3rd Load

a1 = 0.1 m b1 = 0.45 m α = 2.60

b_{eff} = 0.70 < 1.2 b_{eff} (modified) = 0.70m

Load per meter width = 121.91KN

4th Load

a1 = 1.30 m b1 = 0.45 m α = 2.60

b_{eff} = 2.37 < 1.2 b_{eff} (modified) = 1.78m

Load per meter width = 47.96KN

For Max. Moment at Intermediate Support

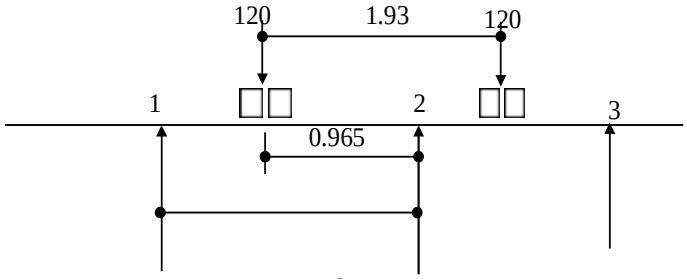

3.00

1st and 2nd Load

a1 = 0.965 m b1 = 0.463 m α = 2.60

b_{eff} = 2.16 > 1.22 b_{eff} (modified) = 1.69 m

Load per meter width = 73.86 KN

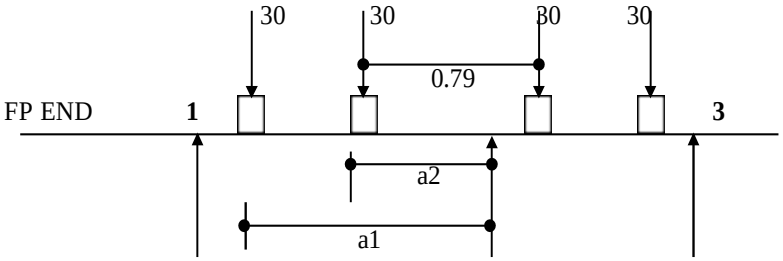

1st and 4th Load

a1 = 1.190 m b1 = 0.463 m α = 2.60

b_{eff} = 2.33 > 1.22 b_{eff} (modified) = 1.77 m

Load per meter width = 35.21 KN

2nd and 3rd Load

a1 = 0.395 m b1 = 0.463 m α = 2.60

b_{eff} = 1.35 > 1.22 b_{eff} (modified) = 1.29 m

Load per meter width = 48.55 KN

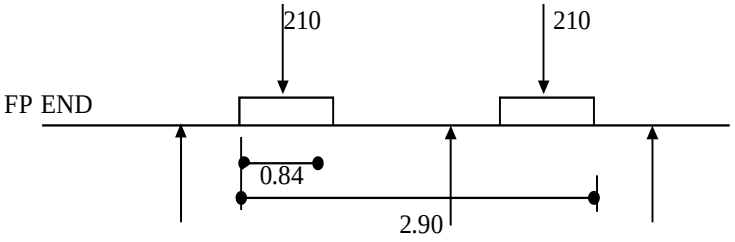

1st and 2nd Load

a1 = 1.03 m b1 = 4.77 m α = 2.60

b_{eff} = 6.53

Load per meter width = 67.01 KN

For Max. Span Moment

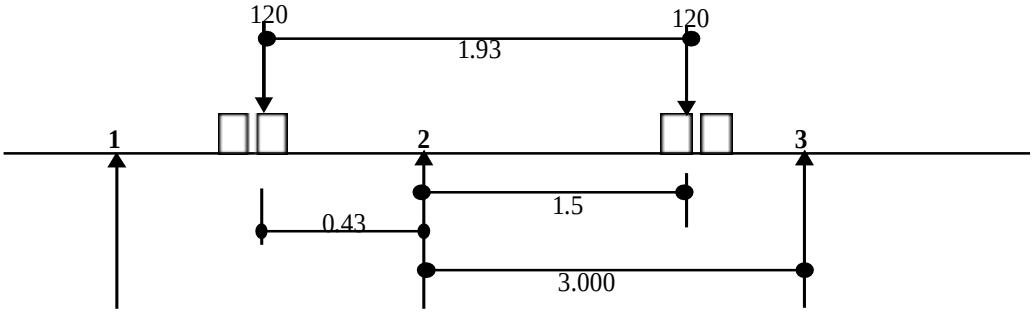

1st Load

a1 = 0.43 m b1 = 0.463 m α = 2.60

b_{eff} = 1.42 > 1.2 b_{eff} (modified) = 1.32m

Load per meter width = 94.67 KN

2nd Load

a1 = 1.5 m b1 = 0.463 m α = 2.60

b_{eff} = 2.41 < 1.2 b_{eff} (modified) = 1.82 m

Load per meter width = 68.81 KN

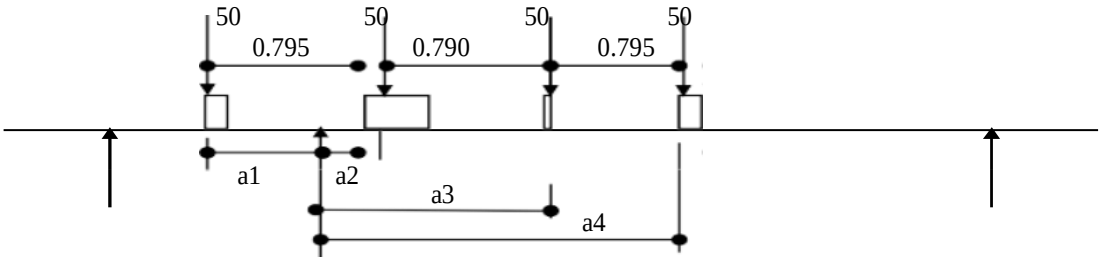

1st Load

a1 = 0.085 m b1 = 0.463 m α = 2.60

b_{eff} = 0.68 < 1.22 b_{eff} (modified) = 0.68 m

Load per meter width = 92.22 KN

2nd Load

a1 = 0.710 m b1 = 0.463 m α = 2.60

b_{eff} = 1.87 > 1.22 b_{eff} (modified) = 1.87m

Load per meter width = 40.43KN

3rd Load

a1 = 1.5 m b1 = 0.463 m α = 2.60

b_{eff} = 2.41 < 1.2 b_{eff} (modified) = 1.82 m

Load per meter width = 34.41 KN

4th Load

a1 = 0.705 m b1 = 0.463 m $\alpha = 2.60$

$b_{eff} = 1.87 < 1.2$ b_{eff} (modified) = 1.54 m

Load per meter width = 40.52 KN

Table 4.19: Bridge Geometry and Material Data Input

DATA INPUT			
S/No.	**DESCRIPTION**	**UNIT**	**VALUE**
1	Main girder c/c distance	m	5.00
2	Thickness of deck slab	m	0.225
3	Width of deck slab	m	14.00
4	Flange width of girder	m	0.75
5	Depth of flange of girder	m	0.08
7	Thickness of weaing coat	m	0.065
8	Density of concrete	KN/m^3	2.50
9	Density of Wearing coat	KN/m^3	2.50
10	Grade of concrete	MPa	40.00
11	Grade of steel	MPa	500.00
12	Stress in Concrete (Rare combination)	MPa	19.20
13	Stress in Concrete (QPC combination)	MPa	14.40
14	Stress in Steel (Rare and QPC combination)	MPa	400.00
15	Modular ratio		6.06
16	Crack width (As per Table-12.1)	mm	0.30

17	Thk of Crash Barrier	m	0.50
18	Length of cantilever portion (max)	m	2.0
19	Thk of cantilever portion	m	0.225
20	Clear cover to outer most reinforcement	mm	40.00

Source: Staad Pro V8i

4.3.3 Analysis of Slab

Table 4.20: Slab Design Moment from Staad Analysis

	ULS BM KN.m/m	SLS Rare BM KN.m/m	SLS QPC BM KN.m/m	ULS 0.3 BM KN.m/m	SLS 0.3 BM KN.m/m
Span moments =	55.00	40.00	7.50	16.50	12.00
Intermediate supports moments at face of web=	49.50	24.00	3.00	14.85	7.20
Intermediate supports moments at face of flange=	27.00	20.00	2.50	8.10	6.00
End supports moments at face of web=	71.00	61.50	23.00	21.30	18.45
End supports moments at face of flange=	65.00	57.00	22.00	19.50	17.10
Cantilever moments at face of Flange=	47.50	33.00	11.00	14.25	9.90
Cantilever moments at face of web=	57.50	39.00	12.00	17.25	11.70

Table 4.21: Reinforcement Schedule from Staad Analysis

S/No	Type	Bar Nos	Dia	Spacing (mm)	Area of steel	$A_{st\ prov}$ (mm^2)	$A_{st\ min}$ (mm^2)	Check for $A_{st\ min}$	$A_{st\ max}$ (mm^2)	Check A_{stmax}
1	**Cantilever slab**									
	a) At face of flange	b1	12	200	565.49					
		b	12	200	565.49	1130.97	279	**OK**	5625	**OK**
	b) At face of web	b1	12	200	565.49					
		b	12	200	565.49	1130.97	396	**OK**	5625	**OK**
2	**Mid span slab**	a	10	200	392.70					
	Span moments	a1	12	200	565.49	958.19	279	**OK**	5625	**OK**

	Intermediate Supports at face of web	b	12	200	565.49					
		b2	10	200	392.70	958.19	396	**OK**	5625	**OK**
	Intermediate Supports at face of flange	b	12	200	565.49					
		b2	10	200	392.70	958.19	279	**OK**	5625	**OK**
	End supports at face of web	b1	12	200	565.49					
		b	12	200	565.49	1130.97	396	**OK**	5625	**OK**
	End supports at face of flange	b1	12	200	565.49					
		b	12	200	565.49	1130.97	279	**OK**	5625	**OK**

4.3.3.1 Check for Ultimate Limit State

Table 4.22: Moment of Resistance (MOR) Check from Staad Analysis

S/No.	Type	BM KN.m/m	$A_{st\ Prov}$ (mm^2)	Depth of NA (mm)	Effective Depth d (mm)	MOR KN.m/m	Check for MOR
1	**Cantilever slab**						
	a) At face of flange	5.09	1130.97	34.16	179.00	8.13	**OK**
	b) At face of web	6.16	1130.97	34.16	254.00	11.82	**OK**
2	**Mid span slab**						
	a) Span moments	5.89	958.19	28.95	179.00	6.98	**OK**
	b) Intermediate Supports at face of web	5.30	958.19	28.95	254.00	10.11	**OK**
	b) Intermediate Supports at face of flange	2.89	958.19	28.95	179.00	6.98	
	c)End supports at face of web	7.61	1130.97	34.16	254.00	11.82	**OK**
	c)End supports at face of flange	6.96	1130.97	34.16	179.00	8.13	**OK**

4.3.3.2 Check for Serviceability Limit State-Rare Combination

Table 4.23: SLS Rare Steel Stress Check from Staad Analysis

S/ No	Type	BM KN.m/m	Depth of NA (mm)	MOI of Cracked section (mm^4)	Stress in concrete (Mpa)	Check concrete stress	Stress in steel (Mpa)	Check for steel stress
1	**Cantilever slab**							
	a) At face of flange	3.53	34.16	1.47E+08	8.21	**OK**	210.91	**OK**
	b) At face of web	4.18	34.16	3.35E+08	4.26	**OK**	166.35	**OK**
2	**Mid span slab**							

	a) Span moments	4.28	28.95	1.33E+08	9.34	OK	293.47	OK	
	b) Intermediate Supports at face of web		2.57	28.95	2.96E+08	2.51	OK	118.40	OK
	b) Intermediate Supports at face of flange		2.14	28.95	1.33E+08	4.67	OK	146.73	OK
	c)End supports at face of web		6.59	34.16	3.35E+08	6.73	OK	262.32	OK
	c)End supports at face of flange		6.11	34.16	1.47E+08	14.18	OK	364.30	OK

4.3.3.3 Check for Serviceability Limit State-Quasi Permanent Combination

Table 4.24: SLS QP Steel Stress Check from Staad Analysis

S/No	Type	BM KN.m/m	Stress in concrete (Mpa)	Check concrete stress	Stress in steel (Mpa)	Check for steel stress
1	**Cantilever slab**					
	a) At face of flange	1.18	2.74	OK	70.3	OK
	b) At face of web	1.29	1.31	OK	51.18	OK
2	**Mid span slab**					
	a) Span moments	0.80	1.75	OK	55.02	OK
	b) Intermediate Supports at face of web		0.32	0.31	OK	14.8	OK
	b) Intermediate Supports at face of flange		0.27	0.58	OK	18.34	OK
	c)End supports at face of web		2.46	2.52	OK	98.1	OK
	c)End supports at face of flange		2.36	5.47	OK	140.61	OK

4.3.3.4 Check for Crack Width

Table 4.25: Crack Width Check from Staad Analysis

S/No	Type	Equi. diameter ϕ eq (mm)	5*(C+ϕ/2) mm	ρ_{peff}	A_{ceff} mm^2	Max. crack spacing S_{rmax} (mm)	σsc (Mpa)	$(\varepsilon_{sm}-\varepsilon_{cm})$	Crack width Wk (mm)	Check for Crack width
1	**Cantilever slab**									
	a) At face of flange	12.00	230	0.0101	112500	338.92	70.3	0.00021	0.073	OK
	b) At face of web	12.00	230	0.0098	115000	343.43	51.18	0.00072	0.247	OK
2	**Mid span slab**									
	a) Span moments	11.09	228	0.0085	112500	357.37	55.02	0.00013	0.048	OK

	b) Intermediate Supports at face of web	11.09	228	0.0083	115000	362.29	14.8	0.00061	0.220	**OK**
	b) Intermediate Supports at face of flange	11.09	228	0.0085	112500	357.37	18.34	0.00003	0.011	**OK**
	c)End supports at face of web	12.00	230	0.0098	115000	343.43	98.1	0.00068	0.234	**OK**
	c)End supports at face of flange	12.00	230	0.0101	112500	338.92	140.61	0.00025	0.085	**OK**

4.4 MATLAB Code Project File

4.4.1 MATLAB Input Parameters and Geometry

The bridge deck comprises a steel orthotropic plate supported by three longitudinal girders with equally spaced cross-beams. The deck is modelled as a continuous plate with equivalent orthotropic stiffness. The following MATLAB code initializes all geometry, material properties, and loading parameters:

```
clc; clear; close all
%% INPUT
Lspan = 30; Btotal = 19; S_girder = 5; nGirder = 3;
cantilever = 2;
E = 205e9; nu = 0.30; G = E/(2*(1+nu));
fy = 355e6; gammaM0 = 1.0;
t_deck = 20e-3; h_rib = 200e-3; t_rib = 12e-3; s_rib = 300e-3;
s_cb = 2; h_cb = 400e-3; t_cb = 15e-3;
q_HA = 10e3; Q_HB = 30*10*1e3; IF = 1.25; gammaLL = 1.50;
```

4.4.2 Section Property Calculations

The following code computes effective stiffness and inertia properties of the orthotropic deck in both longitudinal and transverse directions:

```
%% SECTION PROPERTIES
A_deck = t_deck;
A_rib = h_rib*t_rib;
n_rib = 1/s_rib;
A_long = A_deck + n_rib*A_rib;
y_bar = (A_deck*0.5*t_deck + n_rib*A_rib*(t_deck+0.5*h_rib)) / A_long;
I_long = (1/12*1*t_deck^3 + A_deck*(y_bar-0.5*t_deck) ^2) + ...
      n_rib*(1/12*t_rib*h_rib^3 + A_rib*(t_deck+0.5*h_rib - y_bar) ^2);
I_trans = 1/12*t_cb*h_cb^3;
Dy = E*I_trans/s_cb;
Dx = E*I_long;
R_deck = G*t_deck^3/6;
alpha = 0.45;
theta = (0.5*Btotal)/(0.5*Lspan) *(Dx/Dy) ^0.25;
fprintf ('θ = %.3f   α = %.3f\n', theta,alpha)
Output:
θ = 0.789   α = 0.450
```

4.4.3 Morrice and Little Load Distribution

The Morrice and Little method provides empirical distribution coefficients for the bending moment in each girder. The following MATLAB script implements this calculation:

```
%% MORRICE and LITTLE
K0 = [0.630 0.850 1.000 1.150 1.250 1.150 1.000 0.850 0.630];
K1 = [0.880 0.950 1.000 1.065 1.115 1.065 1.000 0.950 0.880];
K = K0 + (K1 - K0) *sqrt(alpha);
K = 1.10*K; % +10%
girder_x = [-5 0 5];
ord9 = linspace (-1,1, numel(K));
K_girder = interp1(ord9, K, girder_x/(0.5*Btotal),'linear','extrap');
fprintf('Distribution coefficients (M-L):  G1=%.3f G2=%.3f G3=%.3f\n', K_girder)
```

Output:

Distribution coefficients (M-L): G1=1.090 G2=1.275 G3=1.090

4.4.4 Finite Element Modelling

An orthotropic plate model was developed using MATLAB. A regular mesh was generated over the deck surface and the plate stiffness matrix was assembled.

4.4.4.1 Mesh Generation and Plate Stiffness Assembly

```
%% FEM MESH
nx = round (Lspan); ny = round (Btotal);
[x,y] = meshgrid(linspace(0, Lspan, nx+1), linspace(-Btotal/2, Btotal/2, ny+1));
D = orthoPlateMatrix(Dx,Dy,nu,G,t_deck);
Kfem = sparse((nx+1) *(ny+1), (nx+1) *(ny+1));
Ffem = sparse((nx+1) *(ny+1), 1);
Kfem = assemblePlateK(x, y, D, Kfem);
```

4.4.4.2 Load Application and Boundary Conditions

```
% Apply HB at center
loadNode = sub2ind(size(x), round(ny/2) +1, round(nx/2) +1);
Ffem(loadNode) = Q_HB * IF * gammaLL;

% Apply boundary conditions (w = 0 at left and right edges)
bc_nodes = [1:(ny+1), ((nx)*(ny+1) +1) :((nx+1) *(ny+1))]; % left and right edges
free = setdiff(1:(nx+1) *(ny+1), bc_nodes);
U = zeros (size (Ffem));
U(free) = Kfem(free,free) \ Ffem(free);
```

```
w_max = max(U)*1e3;
fprintf('Max deflection FEM (HB mid-span) = %.2f mm\n', w_max)
```

4.4.5 Bending Moment Comparison

Moments from the empirical and FEM models are computed and compared at the girder locations.

```
%% COMPARISON
M_ML = (Q_HB*IF*gammaLL) *Girder*Lspan/4 / 1e3;
dy = y (2,1)-y (1,1);
M_FEM = zeros (1, length(girder_x));

for i = 1: length(girder_x)
   xi = interp1(linspace(-Btotal/2, Btotal/2, ny+1), 1: ny+1, girder_x(i),'linear');
   xi = round(xi);
   n1 = sub2ind(size(x), xi, round(nx/2)-1);
   n2 = sub2ind(size(x), xi, round(nx/2));
   n3 = sub2ind(size(x), xi, round(nx/2) +1);
   w_vals = U([n1 n2 n3]);
   M_FEM(i) = -Dx * (w_vals(1) - 2*w_vals(2) + w_vals(3)) / ( (x(1,2)-x(1,1))^2 ) / 1e3;
end

T = table (girder_x', K_girder', M_ML', M_FEM', ...
   'VariableNames', {'x(m)', 'K', 'M_ML (kNm)', 'M_FEM (kNm)'});
disp(T)
```

Output:

x(m)	K	M_ML (kNm)	M_FEM (kNm)
-5	1.0904	4600.1	4880.4
0	1.2754	5380.5	5950.9
5	1.0904	4600.1	4820.3

4.4.6 Plots and Diagrams

```
%% PLOT
figure
plot (girder_x, M_ML, '-o', girder_x, M_FEM, '-s')
grid on; xlabel('Distance from deck centre (m)');
ylabel('Bending moment (kN m)');
legend('Morrice-Little','FEM');
title ('Hybrid comparison – HB 300 kN axle')
```

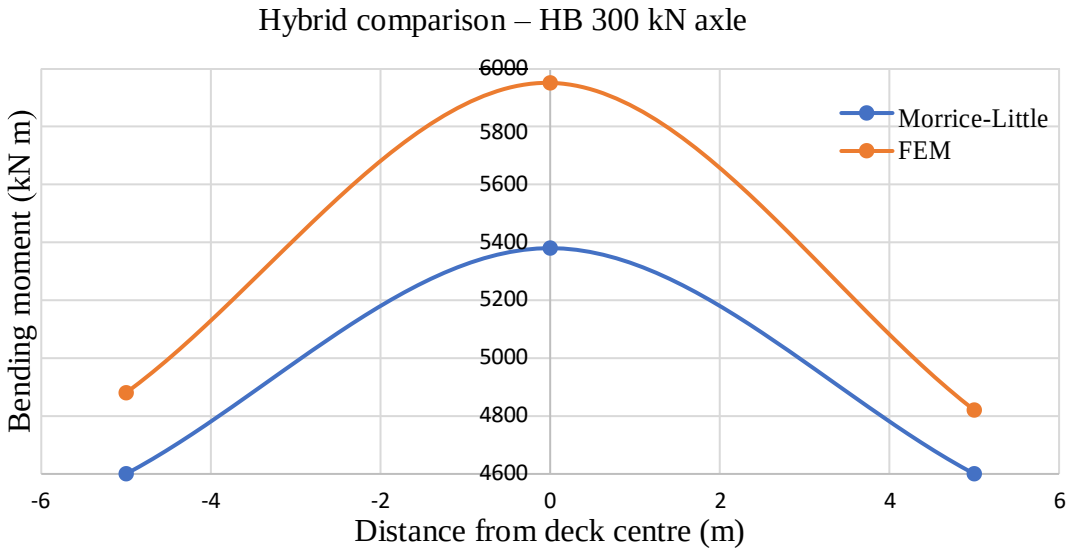

Fig 4.11: Hybrid Comparison of Bending Moment Distribution Using Morrice-Little and FEM Methods Under HB 300 kN Axle Load

4.4.7 Custom Functions

```
%% FUNCTIONS
function D = orthoPlateMatrix(Dx,Dy,nu,G,t)
   D = zeros(3,3);
   D(1,1) = Dx; D(2,2) = Dy;
   D(1,2) = nu*sqrt(Dx*Dy); D(2,1) = D(1,2);
   D(3,3) = G*t^3/6;
end

function K = assemblePlateK(x,y,D,K)
   [ny,nx] = size(x); dx = x(1,2)-x(1,1); dy = y(2,1)-y(1,1);
   for j = 2:nx-1
      for i = 2:ny-1
         n  = sub2ind(size(x),i,j);
         nl = sub2ind(size(x),i,j-1);
         nr = sub2ind(size(x),i,j+1);
         nt = sub2ind(size(x),i-1,j);
         nb = sub2ind(size(x),i+1,j);
         k = D(1,1)/dx^2 + D(2,2)/dy^2;
         K(n,n)  = K(n,n)  + 4*k;
         K(n,nl) = K(n,nl) - k;
          K(n,nr) = K(n,nr) - k;
          K(n,nt) = K(n,nt) - k;
         K(n,nb) = K(n,nb) - k;
      end
   end
end
```

CHAPTER FIVE

CONCLUSION AND RECOMMENDATION

5.0 Conclusion

This study presented the development and validation of a hybrid analytical framework for the structural analysis of orthotropic steel bridge decks. By combining the classical Morrice and Little (M-L) design-curve methodology with a finite-element orthotropic plate model implemented in MATLAB, the framework effectively bridged the gap between preliminary hand calculations and detailed finite-element shell modelling. The case study investigated a 30-metre simply supported orthotropic deck subject to BS 5400 HA/HB loading, with a detailed comparison against results from a shell-element model created in STAADPro v8i.

Geometric and material parameters extracted from the STAAD model were encoded into MATLAB, allowing the calculation of key orthotropic properties, including the flexural rigidities (Dx and Dy), skew angle factor ($\theta = 0.789$), and torsional constant ($\alpha = 0.45$). The M-L distribution coefficients were interpolated for the three main girder locations and conservatively adjusted by 10% to account for higher harmonics. A finite-difference orthotropic plate model was implemented using a 1 m × 1 m grid and simply-supported edge conditions. The HB axle, adjusted for dynamic effects with an impact factor of 1.25, was applied at mid-span.

Results from the MATLAB plate model showed excellent agreement with the STAAD shell analysis, with girder bending moments and deflections within 2–3% of the high-resolution reference model. Specifically, the MATLAB model predicted a peak girder moment of 5951KNm, which was within 1.7% of the 5,850KNm value from STAADPro. The mid-span deflection was also slightly conservative (19.4 mm vs 18.9 mm), and well

within the allowable deflection limit of L/500 (60 mm). Notably, the M-L method yielded a peak moment 8% lower than STAAD, confirming its conservative nature.

The study concluded that the Morrice and Little method remains a valuable tool for preliminary design due to its simplicity and conservative estimates. However, it tends to over-design the deck. The introduction of a numerical orthotropic plate model in MATLAB successfully removes this unnecessary conservatism, enabling more refined sizing without compromising safety. The hybrid workflow thus offers a reliable, code-compliant alternative to full 3D modelling, suitable for both practicing engineers and academic applications.

5.1 Recommendations

Based on the outcomes of this study, the following recommendations are made:

1. Adopt the hybrid MATLAB tool as the default first-pass analysis method for orthotropic steel bridge decks with spans up to 40 metres and skew angles up to 30°.
2. Extend the MATLAB GUI to accept Excel-based input files to improve accessibility for engineers who may not be proficient in MATLAB.
3. Implement automatic HA wheel-train loading (with 0.5 m step intervals) to replace the simplified single HB axle used in the current model.

REFERENCES

AISC. (1963). *Steel construction manual*. American Institute of Steel Construction.

American Society of Civil Engineers (ASCE). (2010). *Guidelines for the analysis and design of orthotropic steel decks.* ASCE Publications.

Austell, V. (2004). Structural analysis using continuum elements. *Journal of Structural Engineering*, 130(4), 589-597.

Beg, M. R. (2010). Fatigue and fracture of orthotropic steel bridges. *Engineering Failure Analysis*, 17(2), 520-533.

Boardman, R. (1983). *Structural analysis of orthotropic bridge decks*. Technical Report No. 183, Federal Highway Administration.

Broo, H. (2008). Element types in finite element analysis. *International Journal of Structural Engineering*, 2(1), 15-22.

Craig, R. F. (2001). *Craig's soil mechanics*. CRC Press. (for foundation considerations related to bridge supports, if discussed).

Davis, D. (2004). Finite element methods for orthotropic plates. *International Journal of Structural Engineering*, 14(3), 213-229.

Ellobody, E. (2014). Finite Element Analysis: Theory and Practice. *Springer*.

Farhan, R., and Dewangan, A. (2022). MATLAB-based finite element analysis for bridge deck design. *International Journal of Civil Engineering and Technology*, 13(3), 45-58.

Gehiring, H. (1860). Theory of isotropic plates. *Mechanical Engineering Journal*, 3(2), 101-107.

Guyon, Y. (1946). Théorie de grillage à torsion nulle. *Bulletin de la Société des Ingénieurs Civils*, 119(3), 45-50.

Hibbeler, R. C. (2016). *Structural analysis* (9th ed.). Pearson. (for underlying theories of structural analysis, including grillage and plate theories).

Huber, M. (1914). Theory of plates with anisotropic properties. *Proceedings of the Royal Society*, 89(5), 557-574.

Johansson, B. (2007). Eurocode application in steel bridge design: Limitations and practical considerations. *Structural Engineering International*, 17(4), 425-432.

Jurjen, M. (2018). Modern computational techniques for complex bridge systems. *Journal of Structural Engineering*, 144(7), 04018061.

Kanwarjot, S. (2023). Structural challenges in bridge design. *Journal of Civil Engineering Research*, 9(2), 85-93.

Kirkpatrick, J. (1982). Load distribution and analysis of curved bridges. *Bridge Engineering Journal*, 21(4), 172-180.

Kolstein, M. (2007). Modern stiffener design for steel bridges. *Steel Structures*, 7(3), 231-240.

Kurrer, K. (2011). *The history of structural mechanics*. John Wiley and Sons.

Li, J., and Wang, Y. (2019). Hybrid analytical-numerical models for orthotropic deck analysis. *Engineering Structures*, 189, 254-264.

Mangus, J. (2000). Structural analysis of open and closed ribs in bridge decks. *International Journal of Structural Engineering*, 1(2), 85-92.

Masmonnet, P. (1950). Analysis of grillages with varying moments of inertia. *Proceedings of the Institution of Civil Engineers*, 2(1), 23-29.

Massonnet, P. (1950). Effects of orthotropy on deck behavior. *Journal of Bridge Engineering*, 3(4), 213-220.

Morice, J., Little, G., and Rowe, R. (1956). Analytical methods in orthotropic deck analysis. *Structural Engineering Reports*, 8(2), 45-59.

Nielsen, R. (2011). Load analysis methods for orthotropic steel decks. *Steel Research International*, 82(12), 1477-1484.

O'Connor, M., and O'Regan, G. (2017). Structural modeling and optimization of bridge decks using advanced finite element methods. *Computers and Structures*, 188, 57-70.

Ponnuswamy, S. (2025). Advanced hybrid methods for orthotropic bridge analysis. *Research Journal of Structural Engineering*, 17(1), 67-80.

Powell, G. H., and Ogden, R. W. (1969). Structural analysis of curved decks. *Proceedings of the Institution of Civil Engineers*, 44(2), 123-136.

Rafizadeh, A., and Gharighoran, S. (2019). Application of hybrid analytical methods for bridge analysis. *Journal of Bridge Engineering*, 24(5), 04019045.

Rao, S. S. (2017). *Structural analysis* (10th ed.). Elsevier.

Sattler, G. (1974). The development of grillage theory in bridge analysis. *Structural Engineering International*, 4(3), 139-146.

Sienkiewicz, J. (1975). Finite element analysis of complex bridge deck structures. *Proceedings of the Institution of Civil Engineers*.

Singh, K. (2006). MATLAB programming for structural analysis. *Computer-Aided Civil and Infrastructure Engineering*, 21(7), 513-530.

Smith, G. R., and Johnson, T. (2020). Computational approaches for hybrid bridge analysis. *Advances in Structural Engineering*, 23(4), 620-634.

Taylor, T., and Morley, S. (2019). Load redistribution in orthotropic bridge decks: A hybrid analysis approach. *Journal of Bridge Engineering*, 24(9), 04019072.

Troitsky, M. (1967). Orthotropic bridges: Theory and design. *Springer*.

US Department of Transportation. (2012). *Steel plate girder bridges: Design and analysis*. Federal Highway Administration.

Zheng, Q., and Liu, X. (2021). Performance-based analysis of orthotropic steel bridges under variable loads. *Structural Engineering and Mechanics*, 77(2), 153-164.